CAPITAL UNIVERSITY OF SCIENCE AND TECHNOLOGY, ISLAMABAD

Damage Assessment of an Existing Reinforced Concrete Frame Structure using Performance Based Seismic Design

by

Sarfraz Ahmad

A thesis submitted in partial fulfillment for the degree of Master of Science

in the

Faculty of Engineering
Department of Civil Engineering

2020

This work is dedicated to my lovely parents who helped me throughout my life. This work is dedicated to my honorable teachers who guided me to face the challenges of life with patience and courage.

CERTIFICATE OF APPROVAL

Damage Assessment of an Existing Reinforced Concrete Frame Structure using Performance Based Seismic Design

by

Sarfraz Ahmad

(MCE163022)

THESIS EXAMINING COMMITTEE

S. No.	Examiner	Name	Organization
(a)	External Examiner	Engr. Dr. Tahir Mehmood	Comsats, Islamabad
(b)	Internal Examiner	Engr. Dr. Majid Ali	CUST, Islamabad
(c)	Supervisor	Engr. Dr. Munir Ahmed	CUST, Islamabad

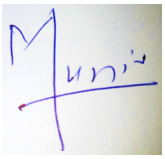

Supervisor Name
Engr. Dr. Munir Ahmed
June, 2020

Dr. Engr. Ishtiaq Hassan
Head
Dept. of Civil Engineering
June, 2020

Dr. Imtiaz Ahmad Taj
Dean
Faculty of Engineering
June, 2020

Author's Declaration

I, **Sarfraz Ahmad** hereby state that my MS thesis titled "**Damage Assessment of an Existing Reinforced Concrete Frame Structure using Performance Based Seismic Design**" is my own work and has not been submitted previously by me for taking any degree from Capital University of Science and Technology, Islamabad or anywhere else in the country/abroad.

At any time if my statement is found to be incorrect even after my graduation, the University has the right to withdraw my MS Degree.

(Sarfraz Ahmad)
Registration No: MCE163022

Plagiarism Undertaking

I solemnly declare that research work presented in this thesis titled "**Damage Assessment of an Existing Reinforced Concrete Frame Structure using Performance Based Seismic Design**" is solely my research work with no significant contribution from any other person. Small contribution/help wherever taken has been dully acknowledged and that complete thesis has been written by me.

I understand the zero tolerance policy of the HEC and Capital University of Science and Technology towards plagiarism. Therefore, I as an author of the above titled thesis declare that no portion of my thesis has been plagiarized and any material used as reference is properly referred/cited.

I undertake that if I am found guilty of any formal plagiarism in the above titled thesis even after award of MS Degree, the University reserves the right to withdraw/revoke my MS degree and that HEC and the University have the right to publish my name on the HEC/University website on which names of students are placed who submitted plagiarized work.

(Sarfraz Ahmad)
Registration No: MCE163022

Acknowledgements

First and foremost, I express my humble gratitude and praise to **ALMIGHTY ALLAH (SWT)**, the creator of universe, who is beneficent and merciful, guide in difficult and congeal circumstances and never leave alone even in the hardest of times, who endow with the will to undertake this project. Next to Him, peace, blessing and great respect to our **Holy Prophet Hazrat Muhammad** , who is forever a beacon of light and knowledge for humanity as a whole, taught us the way to live a productive life.

I would like to pay my special thanks to my respective teacher; lenient and cooperative project advisor **Associate Professor Dr. Engr. Munir Ahmed** who really paid his special attention in the completion of this project. Without his constant help, deep interest, support and vigilant guidance, the completion of this thesis would not be possible.

Last but not the least, I extend my heartily feeling of thanks to my family and friends, for their prayers, support, guidance and encouragement to complete my research project.

(Sarfraz Ahmad)
Registration No: MCE163022

Abstract

Earthquake is one of the many nature's most unpredictable and catastrophic events. In last few decades, many devastating earthquakes have occurred around the world that caused a lot of financial and social loss. The overall goal of this study is to set a methodology for assessment of damages which may occur for a certain level of an earthquake. The study specifically aims at the estimation of structural damages and cost and time to restore the structure to be functional again. For this, an existing 7-storey reinforced concrete building is first designed as per provisions of code UBC-1997. A non-linear model of the building is then created in SAP 2000 software by assigning auto and fiber hinges at physically admisible locations. The model is analyzed by non-linear static push over procedure of FEMA-356 at different intensities of earthquake i.e. Service Level Earthquake (SLE), Design Based Earthquake (DBE) and Maximum Considered Earthquake (MCE). Crack width is choosen as enigineering demand parameter and is determined from the steel strain in re-bars of the structural componant. The crack width is then related to level of damage using damage percentage approach. Extent of damage as well as repair cost and time is estimated in accordance to actual market practices. Repair techniques suggested for the current research study is described in details. A comparison of seismic response parameters for Equivalent Static Analysis (ESA) and Push-over Analysis (PoA) is made and results are discussed. The results give an insight and helped in better understanding of the seismic behaviour of the structure. The relative structural cost comparison show that the repair cost at SLE, DBE, and MCE comes out to be 14%, 17% and 26% of the grey structure construction cost, respectively. The time durations for repair works, based on a team of 3 technical persons working for 8 hours per working day, is estimated 62, 67, and 74 days for SLE, DBE, and MCE, respectively. The results of seismic response parameters and only 26% repair cost even at MCE show that ESA and Code Based Seismic Design (CBSD) procedures are conservative in many ways and underestimate the capacity and seismic behavior of the structure. Therefore, it is need of the hour to switch from linear static to nonlinear static/-dynamic analysis procedures to get more rational, realistic and economic solutions

in order to achieve the desired performance objectives. The study will be helpful for researchers and designers for estimation of structural damages of proposal and existing buildings. The effect of non-structural members to assess the extent of damage using non-linear time history analysis is, however, needed to be explored.

Contents

List of Figures

List of Tables

Abbreviations

ACI	American Concrete Institute
ASCE	American Society of Civil Engineering
ATC	Applied Technology Council
BCP	Building Code of Pakistan
CBSD	Code Based Seismic Design
CFRP	Carbon Fiber Reinforced Polymer
CoM	Center of Mass
CoR	Center of Rigidity
CP	Collapse Prevention
CSI	Computer Structures International
CTBUH	Council on Tall Buildings and Urban Habitat
DBE	Design Based Earthquake
DI	Damage Index
EC8	Euro Code 8
EDP	Engineering Demand Parameter
ESA	Equivalent Static Analysis
EQ	Earthquake
FEMA	Federal Emergency Management Agency
FEM	Finite Element Modelling
IBC	International Building Code
ICC PC	International Code Council, Performance Code
IDR	Interstorey Drift Ratio
IO	Immediate Occupancy
LDP	Linear Dynamic Procedure

LSP	Linear Static Procedure
LS	Life Safety
MCE	Maximum Considered Earthquake
MDoF	Multiple Degree of Freedom
MDR	Mean Damage Ratio
NDP	Nonlinear Dynamic Procedure
NEHPR	National Earthquake Hazards Reduction Program
NSP	Nonlinear Static Procedure
OSDI	Overall Structure Damage Index
PBEE	Performance Based Earthquake Engineering
PBSD	Performance Based Seismic Design
PC	Plain Concrete
PGA	Peak Ground Acceleration
PGD	Peak Ground Displacement
PGV	Peak Ground Velocity
PoA	Push-over Analysis
RC	Reinforced Concrete
RSA	Response Spectrum Analysis
SDoF	Single Degree of Freedom
$\mathbf{S}_D$	Stiff Soil
SLE	Service Level Earthquake
UBC	Uniform Building Code

Symbols

f'_c	Compressive Strength of concrete
f_y	Yield strength of steel
A_g	Gross cross-sectional area
A_e	Effective area of concrete
A_s	Area of steel
P_u	Factored axial load
K	Stiffness of structure / structure member
E	Modulus of elasticity
M_y	Yield moment
M_u	Ultimate moment
σ	Concrete stress
ε	Concrete strain
D	Dead load
L	Live load
L_s	Live Special
E	Earthquake load
l_p	Plastic hinge length
d_b	diameter of reinforced bar
C_0	Modification factor to relate spectral displacement
C_1	Modification factor to relate expected maximum inelastic displacements to displacements calculated for linear elastic response
C_2	Modification factor o represent the effect of hysteresis shape on the maximum displacement response

C_3	Modification factor to represent the increase displacement due to P-Δ effect
S_a	Spectral acceleration
T_e	Effective time period
g	Acceleration of gravity
R	Response modification factor
w	Maximum crack width
V_E	Elastic base-shear
V_D	Design base-shear
V_I	Inelastic base-shear / Actual base-shear
Δ_t	Target displacement

Chapter 1

Introduction

1.1 Background

Structural damage in a building may occur due to many natural causes; settlement, land-sliding, natural erosion, extreme weather, earthquake, flood, tsunami, volcanic eruption, to name a few. Among them, earthquake is the most unpredictable, catastrophic and frequently occurring event which causes a bulk of social and financial loss in the blink of an eye. Such great financial loss and death rate provoke researchers to deal with mitigating the seismic hazard in countries susceptible to earthquake. In the last few decades, many devastating earthquakes have occurred around the world. The ongoing seismic incidents have prompted concerns on safety and vulnerability of the buildings.

Reinforced concrete (RC) frame buildings are one of the most commonly used and adopted construction styles around the globe. Therefore, it is of prime importance to categorize such buildings that have high vulnerability against an expected earthquake, for reliable loss approximation as well as setting criteria to strengthen the buildings. Assessing the vulnerability of a building as a whole is a difficult task because of unavailability of experimental and observed data. Due to this reason, evaluation of RC buildings in terms of its components is preferred.

The buildings that collapsed during recent earthquakes were found unable to match requirements of modern codes (Poluraju and Rao, 2011). Conventional seismic design codes intend only life ecurity of the inhabitants and collapse prevention of the structure. These codes are made very simple for easy and quick design calculations underestimating many factors. Yet, it is believed that code based seismically designed building shall remain serviceable, life safe, and collapse prevented against service level, design basis, and maximum considered earthquake, respectively (UBC, 1997). Code based design procedure is conservative in a sense that it tells that damage will occur but does not tell where and how much damage will occur. The structures susceptible to earthquake (EQ) damage must be recognized and an adequate level of safety must be determined. Conventional prevailing linear-static analysis methods are found deficient for such assessment (Kadid and Boumrkik, 2008). Recently, a new procedure is introduced by Federal Emergency Management Agency (FEMA-365, 2000) namely Performance Based Seismic Design (PBSD) to address the said issues. PBSD can be used to design new structures as well as to evaluate the performance of the existing structures. PBSD enables the designer to choose the hazard and performance level to attain the desired performance objective of the structure. Performance based analysis assess the performance of a structure at each limit state (Tehranizadeh and Moshref, 2011). PBSD gives reliable, satisfactory, and realistic results. Due to these attributes, PBSD is now recommended for advanced analysis of structures in USA as well as in many other modern countries around the globe (Moehle, 2008; CTBUH, 2008).

1.2 Research Motivation and Problem Statement

It is not a usual practice to design earthquake-proof buildings that will not get damaged even for strong but rare ground shaking, as it will result into highly expensive structural systems. Instead, engineering aim is to make earthquake-resistant buildings that can withstand the ground seismic, although they may get severely damaged but would not collapse in a seismic event assuring the security

of the inhabitants and building contents. For economy reasons, the seismic design philosophy is based on allowing damage at specified locations in the structural components such as at beams ends and lower end of the lowest story columns in moment resisting frame systems. On the contrary, building stakeholders in the built environment are now well familiar to the social and financial consequences of earthquake losses and are demanding a viable and practical solution to address the concerns about damage control and loss reduction. Stakeholders of the building, being unaware or not interested in seismic engineering terminologies, are concerned about extent of damage, safety level, and amount of cost and time required to restore the building to be functional. Therefore, effectiveness of PBSD to evaluate the performance and damage occurred in the building needs to be explored. In the current case study, a realistic building is chosen to investigate the seismic behavior and extent of damage occurred at different earthquake levels. Furthermore, cost and time analysis is also done and compared at different earthquake levels.

1.3 Objectives

Different researchers have proposed different techniques for evaluation of damage assessment numerically and experimentally. The overall goal of the study is to set a simple yet practical methodology for seismic damage assessment. For this, an existing multi storey building located in seismic zone 2B and soil type S_D is taken as case study. The key objectives of the current research project are:

1. Evaluation of seismic performance of the case study building.

2. Damage assessment at different hazard levels.

3. Repair cost and time comparison at different hazard levels.

1.4 Scope of Work and Research Methodology

In order to accomplish the goals of the present research work, a real-life 7 storey building located in seismic zone 2B and soil profile type S_D is considered. First, the building is designed using code based design approach. Then, in context to PBSD, non-linear static push-over analysis is performed, as describe in FEMA-356 (2000), to evaluate the seismic performance of the building. Seismic response parameters such as base shear, storey shear, storey moment, storey displacement, and storey drift are calculated and compared in X- and Y-directions for different levels of EQ. Extent of damage is predicted taking crack width as key parameter. Furthermore, cost and time required to repair the damage is also estimated as per current market practices. A total of twelve analysis are performed as detailed in Table 1.1.

TABLE 1.1: Numerical models created for this study

Sr. No.	Model	EQ level	X-direction	Y-direction
1	Code Based Design	SLE	1	1
2	Code Based Design	DBE	1	1
3	Code Based Design	MCE	1	1
4	Push-over Analysis	SLE	1	1
5	Push-over Analysis	DBE	1	1
6	Push-over Analysis	MCE	1	1
		Sub-total	6	6
			Total	12

1.5 Limitations of the Study

The limitations of this research project are:

1. Only the numerical modeling, analysis and design have been done.

2. Only linear equivalent static analysis (ESA) and non-linear static pushover analysis (PoA) have been performed.

3. Non-linearity has been assigned only at specified locations, not throughout the elements and structure.

4. Only super structure has been considered in this study.

5. The effects of non-structural elements have not been taken into account.

1.6 Thesis Outline

CHAPTER 1: In this chapter, research gap has been identified. Motivation and problem statement is discussed. Limitations, scope of work, and research methodology have been outlined.

CHAPTER 2: This chapter gives a detailed literature review presenting different techniques/methods/approaches using various parameters adopted by different researchers for damage assessment. Non-linear static pushover analysis has been discussed.

CHAPTER 3: This chapter includes details about linear and non-linear models created. Modeling and assignment of non-linear hinge property is also explained. A case study of 7 storey building is discussed in detail. First elastic design of intermediate moment resisting frame (IMRF) is performed, and then non-linear design approach is applied.

CHAPTER 4: In this chapter, comparison of different seismic response parameters like storey shear, storey moment, storey displacement, storey drift etc. have been done. Damage assessment and cost and time analysis is performed. Results are drawn and discussed in details.

CHAPTER 5: This chapter covers the summary of the whole research work performed. Conclusions of the research work have been portrayed and future recommendations are presented.

REFERENCES: References of the research papers, research studies and literature used to explore and support the current research project are listed at the end of the thesis.

Chapter 2

Literature Review

2.1 Background

This chapter covers the seismic behavior of reinforced concrete (RC) frame structures and discusses credibility of code based and performance based seismic design. Different techniques and approaches for damage assessment developed by different researchers are presented briefly. Different methods of analysis are explained. FEMA based non-linear static Pushover Analysis (PoA) is reviewed in details.

2.2 Damage Assessment

Damage may be defined as the degradation of the structure's initial capacity in terms of its strength, stiffness and ductility. Earthquake induces highly uncertain lateral force on the structure due to which the structure may get damaged or collapse. Structure must be strong enough to survive the multi hazard effects resulted by the lateral loading (Hait et al., 2020). Corrosion of reinforcement steel rebars is one of the many causes for damage and failure of RC structures (Daniyal and Akhtar, 2020). Zima (2020) studied the damage in RC beams caused by debonding between steel rebars and concrete. Thai et al. (2020) conducted a research regarding damage assessment of RC columns under blast loading.

Vatsikas and Lu (2003) conducted a study to compare code-based (Eurocode 8) and performance-based design procedures regarding initial and life-cycle cost. Initial cost was determined by considering costs of cocnrete, steel and building contents and equipments. Life cycle cost incorporated repair cost, contents loss cost and human fatalities cost. SAP 2000 (CSI, 2006) software was used to generate 4 models of a 8 storied RC building, 3 as per EC8 with different q values and 1 as per PBSD. q is the behaviour factor suggested by EC8, similar to R factor used in U.S. practice, which incorporates the inelastic behaviour of the building. q=1 represents the elastic behaviour of the building and q>1 represents inelastic behaviour of the building.

Interstorey drift raito (IDR) was choosen as engineering demand parameter. The limit values of IDR for immidiate occupancy (IO), life safty (LS), and collapse prevention (CP) levels were 0.25%, 0.75%, and 1.5%, respectively. Each design was examined against frequent, infrequent, and rare earthquakes using nonlinear time history analysis method. Wen and Kang (2001) methodology was adopted for cost analysis. The study concluded that although the initial cost of performance based seismic design (PBSD) was slightly higher but life-cycle cost and total cost of PBSD was much lesser than that of code based design as depicted in Figure 2.1.

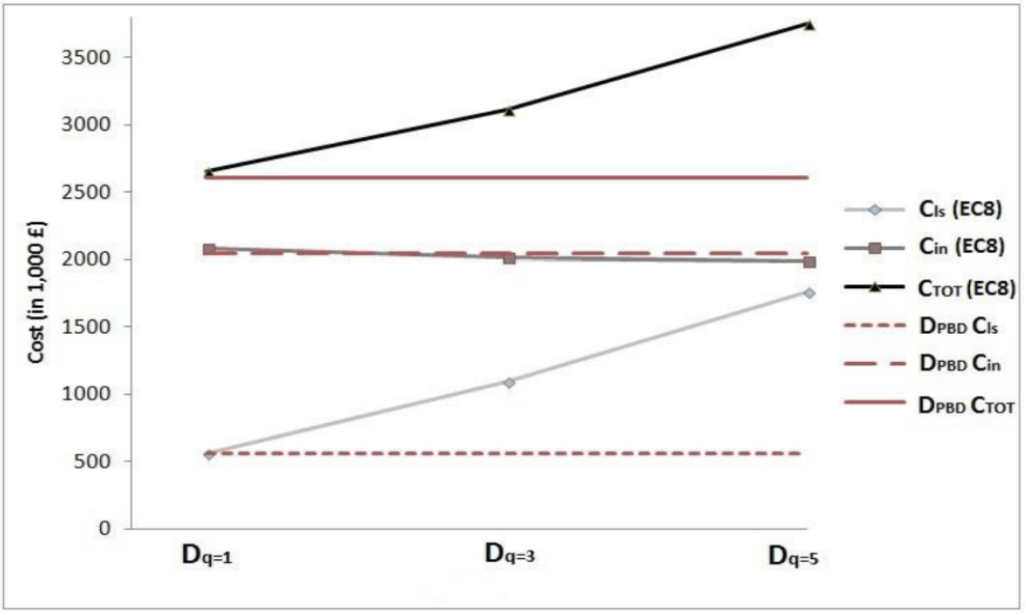

FIGURE 2.1: Initial cost, life-cycle cost and total cost comparison for code based and performance based seismic design (Vatsikas and Lu, 2003)

Simsir et al. (2012) evaluated seismic damage assessment of RC multi-story hotel buildings in Hawaii. The mid-rise buildings containing deficient ductile detailing were designed in 1960s and 1970s and were severely damaged from 2006 earthquakes of Hawaii. Structural properties of buildings were determined from available building plans and on-site observations. Among other structural damages, major damage was caused by cracks in shear walls and tall columns supporting the walls. Cracks were diagonal at lower floors and vertical in upper floors. Crack widths were determined by coring through epoxy injected cracks. Petrographic analysis was also performed on coring samples to evaluate the relative age of cracks. SAP 2000 software was then used to develop 3D-models of various hotel buildings and finite element site specific response spectrum analysis was carried out for determination of stresses caused due to gravity and earthquake loadings. The buildings were designed and analyzed as per provisions of American Society of Civil Engineers (ASCE) 41 (ASCE, 2007). Site specific response spectra was estimated using average spatial weighting technique (King et al., 2004). Results of the computer model analyses correlated well with the observed pattern and direction of cracks in shear walls and columns as portrayed in Figure 2.2. Epoxy injection of cracks as outlined in FEMA-308 (1999) and use of fiber reinforced polymer (FRP) sheets were recommended as repair remedy.

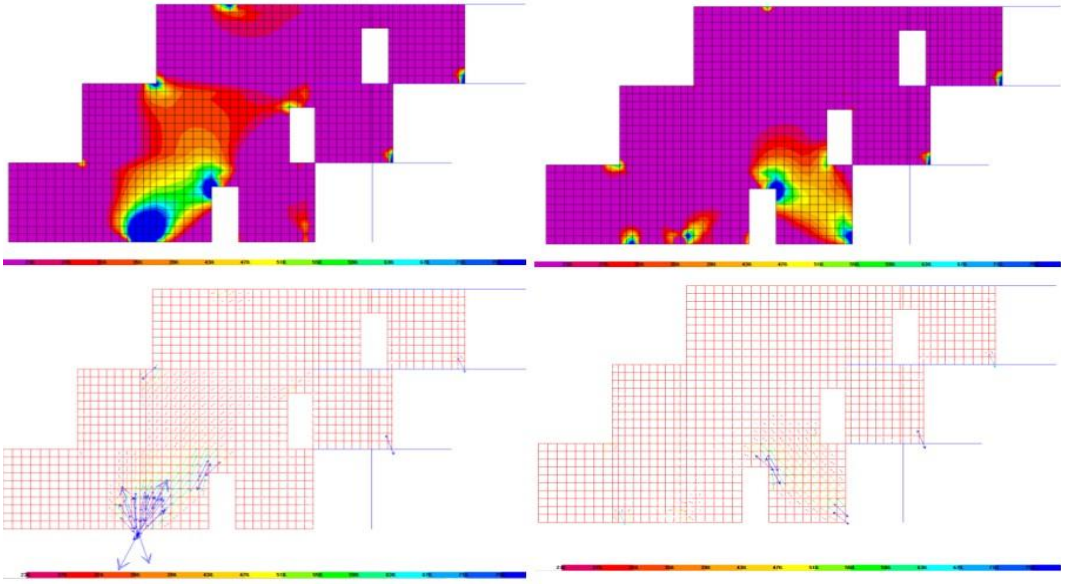

FIGURE 2.2: Stress contours and stress directions in shear walls (Simsir et al., 2012)

Erduran et al. (2012) performed a real-time EQ damage assessment in Romanian-Bulgarian border region. Study was conducted to generate a map to be used by rescue and emergency management agencies critical decision making about how to proficiently utilize the resources for rescue and recovery operations. Analysis was done to approximate the damage for each building as per capacity spectrum method (Freeman et al., 1975, 1978). Assessment was done using HAZUS methodology based SELENA software (Molina et al. 2009, 2010), using shake maps and static input files. Shake maps were generated by shake map server. Damage and loss estimation was done using Mean Damage Ratio (MDR) approach. Four damage states minor, moderate, severe, and complete were defined as per FEMA-445 (2006) and buildings falling under severe and complete damage state were considered to be life-threating. Results of EQ damage assessment were plotted as maps that depicted percentage of buildings that were expected to be in life-threating damage state. One such map that was generated against Vrancea earthquake (1986) having magnitude of 7.1 is shown in Figure 2.3 as an example.

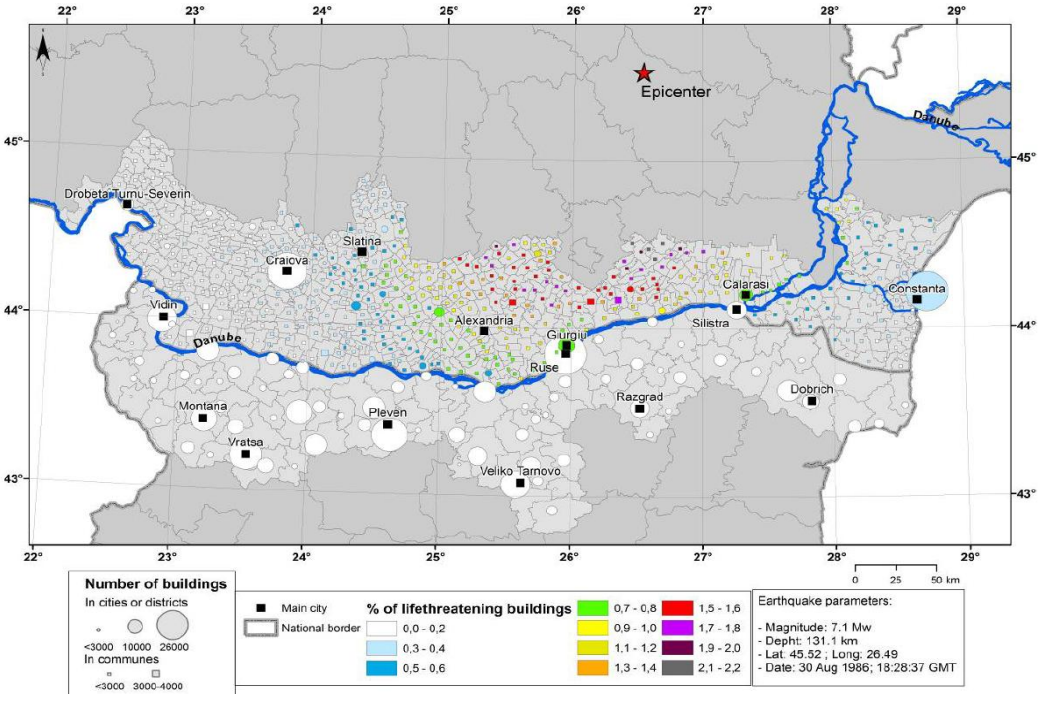

FIGURE 2.3: Final map presenting summary of damage assessment (Erduran et al., 2012)

Elenas and Meskouris (2001) conducted a correlation study between seismic parameters and damage indices of structures. Several seismic parameters like peak ground acceleration (PGA), peak ground velocity (PGV), peak ground displacement (PGD), spectral pseudo-acceleration (SA), spectral pseudo-velocity (SV), spectral displacement (SD), central period (CD), seismic input energy (Einp), Fourier spectra, ARIAS intensity, and HUSID diagram were investigated for correlation with damage indices. An eight story RC frame structure was designed according to the provisions of Eurocodes 2 and 8 (EC2, EC8). Wind and snow loads were considered in addition to dead, live, and seismic loading. After the numerical evaluation of seismic parameters, nonlinear dynamic analyses were conducted to get structural damage states using computer program IDARC (Reinhorn et al. 1996). Among the several seismic parameters, the main focus was on Inter story drift (ISD) and overall structure damage index (OSDI). Limits were set for classification of damage states as low, medium, great, and total as presented in Table 2.1. Results concluded that peak ground motion parameters (PGA, PGV, PGD) give poor or fair correlation with the OSDI, while the spectral (SA, SV, SD) and energy (ARIAS intensity, HUSID diagram) parameters provide good correlation.

Table 2.1: Structural performance level definition (FEMA-356, 2000; ATC-40, 1996; Antoniou, 2002)

	Damage			
	Low	Medium	Great	Total
OSDI	≤ 0.3	0.3<OSDI≤0.6	0.6<OSDI≤0.8	>0.8
ISD (%)	≤0.5	0.5<ISD≤1.2	1.2<ISD≤1.7	>1.7
MEP DI (%)	≤ 0.5	0.5<MEP DI≤1.2	1.2<MEP DI≤1.7	>1.7
Contents DI (g)	≤ 0.2	0.2<Contents DI≤0.8	0.8<Contents DI≤1.25	>1.25

Damage Index (DI) is another useful tool to evaluate the performance of structure and also helps in critical decision making like selection of retrofitting technique for post-earthquake damage. DI value normally ranges from 0 to 1, where 0 represents undamaged state and 1 presents collapsed state. Sinha and Shiradhonkar (2012)

studied the correlation between analytical damage indices and observational damage states. Various damage indices with different parameter values were chosen for two RC buildings. The ability of damage indices in determining undamaged, light, moderate, and collapse damage states of the buildings were explored. Crack width was chosen as a parameter for evaluation of damage state. Maximum crack width was determined by the formula proposed by Gergely and Lutz (1968) as given in Equation 2.1. Sinha and Goyal (2004) definitions for different damage states were set as described in Table 2.2.

$$\text{Wmax} = 0.076\beta f s^3 (dc + Ae)^{0.5} \times 10^{-3} inches - - - Equation(2.1)$$

TABLE 2.2: Damage state definitions for different structural elements (Sinha and Goyal, 2004)

Damage State	Column	Beam
S5	Crushing of core concrete (Crack > 3mm)	Crushing of concrete at supports, heavy deflection
S4	Diagonal cracks in concrete core (0.5mm - 3mm)	Cracks in concrete core (0.5mm - 3mm)
S3	Spalling on outer layer, hairline cracks in core concrete (0.2mm - 0.5mm)	Spalling on outer layer, hairline cracks in core concrete (0.2mm - 0.5mm)
S2	Visible cracks ((0.1mm - 0.2mm)	Visible shear and tension cracks (0.1mm - 0.2mm)
S1	Very fine cracks (<0.1mm)	Very fine cracks (<0.1mm)
S0	No observable damage	No observable damage

IDARC-2D was utilized for analytical modeling of buildings. Non-linear dynamic analysis was conducted using real ground motions of past five earthquakes (ElCentro, Taft, Chile, Chi-chi, and Northridge). It was concluded that most damage indices adequately predict the undamage and collapse damage states of the buildings. However, damage indices were unable to effectively forecast intermediate (minor and moderate) damage states.

Bayuaji et al. (2018) conducted a case study for corrosion damage assessment of a 1500 m long RC canal structure that had been exposed to coastal environment for twenty years using the deterministic approach. Environmental conditions such as average temperature, relative humidity and rainfall intensity were taken into

consideration for case study project. As the structure was exposed to marine environment, chemical composition (pH, sulphate and chloride content) analysis of sea water was also considered for assessment of canal. Visual inspection was done by examining the location and pattern of cracks. Crack width was measured by width detector and crack depth was determined by ultrasonic pulse velocity (UPV) equipment. Field tests included hammer test and UPV test to determine the compressive strength of concrete and half-cell potential test to monitor the corrosion activity of the reforming steel rebars. Core-drilled test was performed to collect concrete samples from different locations on the canal. A number of laboratory tests like compression tests, pH tests, chloride level tests, and rebar tensile test were carried out on the core-drilled samples. Results of laboratory tests showed that the concrete was in good condition having compressive strength more than 85% of the specified compressive strength. No indications of corrosion were found in core-drilled concrete samples. The corrosion initiation time for the canal was calculated to be more than 35 years. It was concluded that no strength degradation had occurred and no strengthening was required upto 2025.

Valente and Milani (2019) conducted a numerical research regarding damage assessment and collapse investigation of 3 ancient palaces under seismic actions. The three palaces, Palazzo Te, Palazzo d'Arco, and Palazzo dell'Accademia, located in Northern Italy were constructed in 1525, 1784, and 1773, respectively and hence of great cultural heritage importance. The core objective of the study was to explore the seismic vulnerability and performance of the palaces after 2012 Emilia earthquakes. The preliminary data was collected through history and documentary research, visual inspections during on-site surveys, and photographic collection of damage and crack patterns in order to better understand the complex geometry and construction typology as well as develop detailed 3-D finite element (FE) models of the palaces. The FE models were created in Abaqus software and non-linear dynamic eigen-frequency analyses, using real accelerograms of 2012 Emilia EQ, were performed to simulate the response of the palaces in case of a seismic event. The analyses were carried out using three values (0.05g, 0.15g, and 0.25g) of peak ground acceleration (PGA) to identify the most vulnerable

elements and predict the damage distribution at different intensities of EQ. For masonry non-linear behavior, concrete damage plasticity (CDP) model was chosen with some alterations of main parameters from literature. Results were drawn and compared in terms of predicted damage distribution, energy density dissipated by tensile damage (EDDTD) and displacement demand. Numerical results and real observed damage correlated well for the research study indicating that the adopted numerical approach can be satisfactorily used to simulate seismic action and response. Among all elements, vaults of all three buildings were identified as the most vulnerable element with extensive damage having highest EDDTD values. The horizontal displacements analysis showed maximum values for external walls of all three palaces. The vertical displacements analysis resulted in probable collapse of the west vaults of Palazzo Te.

It is evident from above discussion that a lot of work has been done by many researchers in the field of seismic damage assessment of frame buildings. In most of the studies, damage assessment by various approaches is done and different repair and strengthening techniques are suggested. However, there is no such study that also approximates the cost and time require to restore the building to be functional, as stakeholders of building, being unaware of seismic engineering terminologies, are more curious about cost and time. In this study, based on knowledge available in literature, market survey, and an assumption, an attempt has been made to estimate the repair cost and time along with damage assessment and remedial suggestion.

2.3 Seismic Assessment of the Structure

The structures, in a seismically active region, need to be designed and evaluated in accordance with modern earthquake engineering tools as the increasing earthquake losses is a burning issue of the present day world. Mostly, an earthquake occurs by sudden rupture or distinctive movement of geological fault (Kramer, 1996). As a result of that, aa tremendous volume of energy is unleashed that travels to earth

surface in the form of waves and produce vibrations. This ground shaking can severely damage and/or collapse buildings and other infrastructure systems. Performance based earthquake engineering (PBEE) is a recent and advanced approach to cope with design and/or assessment of buildings (FEMA-356, 2000; ATC-40, 1996; Themelis, 2008). PBEE is a rational and systematic approach to design a building in such a way that its performance is defined and damage is predictable in case of an earthquake (Guo et al., 2020). Assessing the vulnerability of whole building is a difficult task because of unavailability of experimental and observed data. Due to this reason, evaluation of RC frame structures in terms of its components is prefered. As far as seismic performance is concerned, beams and columns are the most crucial components of a RC frame structure.

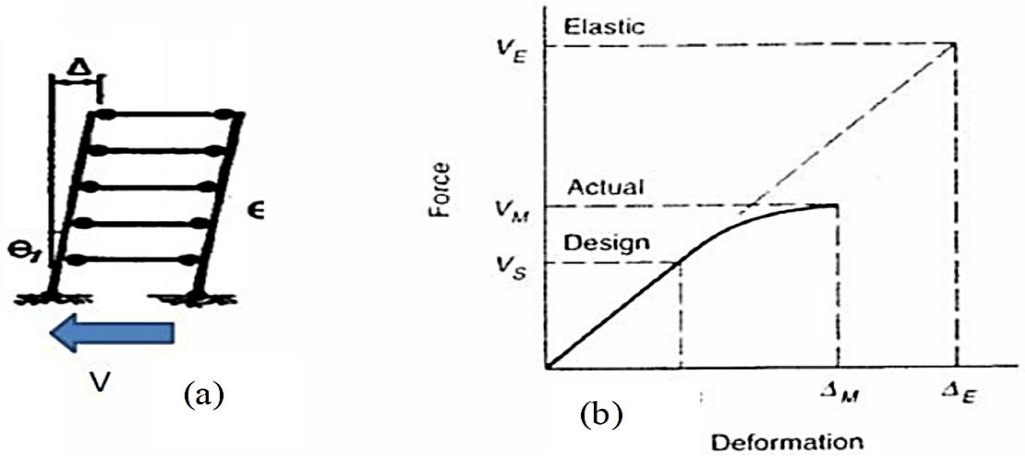

FIGURE 2.4: (a) Seismic design philosophy (b) Assumed force-deformation relationship (Allan Williams, 2000)

For economy reasons, the seismic design philosophy is based on allowing damage at specified locations in the structural elements such as at beams ends and bottom of the lowest story columns in lateral force resisting systems as shown in Figure 2.4a. In both equivalent linear static force and code based response spectrum analysis, this design philosophy is applied using response modification factor/force reduction factor, represented by R (IBC, 2012; UBC, 1997; FEMA-450, 2003; and BCP, 2007). This factor controls the seismic response of structure in case of a seismic event. Figure 2.4b presents the force-deformation relationship when seismic design philosophy is applied to a structure.

Equation 2.2 defines R as ” “the ratio of elastic strength demand (VE) to inelastic design strength (VD) and accounts for over strength and overall ductility of the structure.”” Figure 2.5 illustrates the elastic and inelastic seismic behaviour of the structure.

- The red line shows the linear relationship between force and displacement when the structure responded elastically.

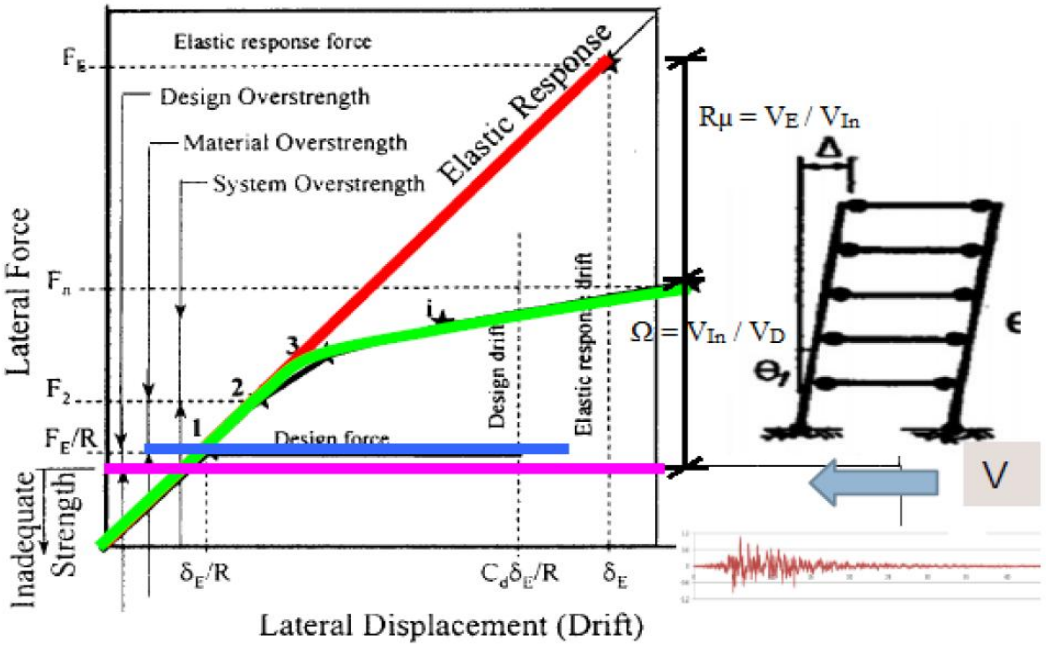

FIGURE 2.5: Elastic vs inelastic seismic behaviour of the structure (Uang, C. M., 1991)

- The green line represents the actual force vs displacement response of the structure.
- The pink line shows the minimum strength that the structure requires for inelastic response.
- The blue line indicates the strength for which the structure is designed.

$$R = V_E \text{ (elastic base-shear)} / V_D \text{ (design base-shear)} \quad ---Equation(2.2)$$

2.4 Equivalent Static Analysis (ESA)

Equivalent static analysis (ESA) is the most commonly used, simple, easy, and quick method for analysis of structures. It is based on the simple concept that a static lateral force equivalent to dynamic force resulted from ground shaking is applied to the structure and then structure is analyzed accordingly. UBC-97 puts a limit for the use of ESA and permits this procedure only when a regular structure is of height upto 240 feet or when an irregular structure is of height upto 65 feet. When the height exceeds more than 240 feet or 65 feet in case of regular or irregular structures, respectively, or when the structure is lying on soil profile type SF with time period of more than 0.7 sec, dynamic response spectrum analysis is recommended. ESA is mostly used for the design of regular structures. For irregular structures dynamic analysis is best suited (Di Julio, R. M., 2001; ACl-318, 2008).

Bourahla (2013) describes ESA as a simplified procedure in which lateral load is distributed over the height of the structure for evaluation in context of effect of dynamic loading of predictable seismic event. The induced seismic force or base shear (V) is evaluated in X- and Y-directions. Precise design can be obtained provided the structure responds in its fundamental lateral mode and is identical in both X- and Y-directions.

2.5 Performance Based Seismic Design (PBSD)

Seismic events around the globe in the last quarter of the 20th century became a reason for collapse or extensive damage of many buildings that were designed in accordance with prevailing codes. The buildings were incapable to withstand the effects of seismic event despite of the fact that safety factors against earthquake had been taken into consideration while designing the structure. The probable reason for this was that there are many restrictions and limitations in code based design techniques. The stockholders of the building had concerns about safety

and damage of the building. The scenario also became a challenge for structural engineers that how to evaluate the vulnerability and damage assessment of existing buildings as well as design of new structures. There was a need for new analysis and design approach. Performance based seismic design (PBSD) emerged as an effective solution.

The fundamental objective of PBSD is to design a building with known approximation of damage in a seismic event. The PBSD approach has been in practice since the performance level of the building in case of earthquake is pre-defined. In PBSD, extent of damage in case of earthquake can be analyzed. In PBSD methodology, two parameters are required to be calculated for analysis and design purposes i.e. seismic capacity and seismic demand (ATC-40, 1996). The seismic capacity is the capability of the building to resist seismic effects whereas; the seismic demand is the earthquake effects imposed to the structure. The structure must be designed in a way that the seismic capacity always exceeds the seismic demand.

The ICC PC (International Code Council, Performance Code, 2012) defines performance based design as, "An engineering approach to design elements of a building based on agreed upon performance goals and objectives, engineering analysis and quantitative assessment of alternatives against the design goals and objectives using accepted engineering tools and methodologies". The step-wise procedure for ICC PC of buildings is shown in Figure 2.6.

A performance objective is a combination of two components called hazard level and performance level as detailed in Table 2.3 and Table 2.4, respectively. Association of performance level with a hazard level is called a performance objective. The leading advantage of PBSD is that any performance objective can be achieved when the structure is subjected to any specified hazard level. Figure 2.7 illustrates the performance levels of a building as per FEMA 273/356 along with tentative expected approximate repair cost and time.

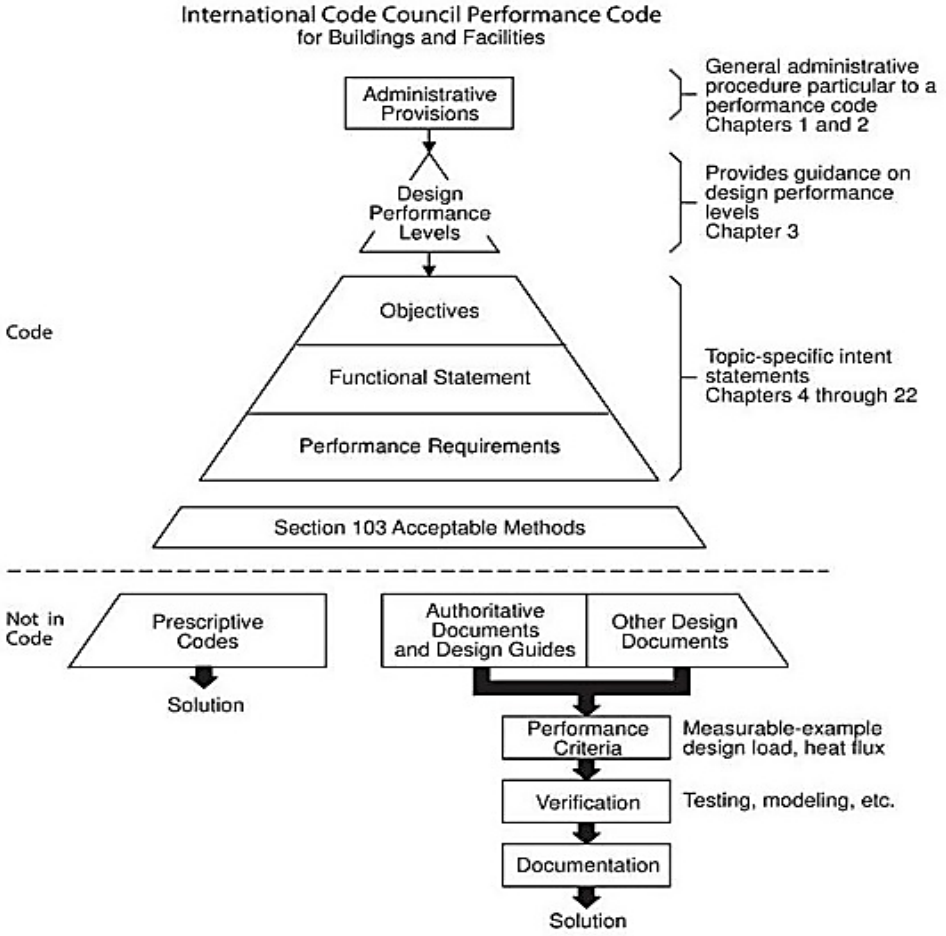

FIGURE 2.6: Outline for ICC PC (2012)

TABLE 2.3: Structural hazard level definition (FEMA-356 2000; ATC-40, 1996)

Hazard Level	Description
Frequent, minor EQ (SLE)	Return period: 100 years (43% probability of occurrence in 50 years)
Infrequent, moderate EQ (DBE)	Return period: 500 years (10% probability of occurrence in 50 years)
Worst EQ ever likely to occur (MCE)	Return period: 2500 years (2% probability of occurrence in 50 years)

TABLE 2.4: Structural performance level definition (FEMA-356, 2000; ATC-40, 1996; Antoniou, 2002)

Performance Level	Description
Operational (O)	Negligible impact on building. Building can be occupied. No repair work required.
Immediate Occupancy (IO)	Building is safe to occupy but will need little repair work.
Life Safety (LS)	Building is safe during the event but possibly not afterward. Building can be occupied after subsequent repair.
Collapse Prevention (CP)	Building is on the verge of collapse, probable total loss. Building is far beyond the economically feasible repair.

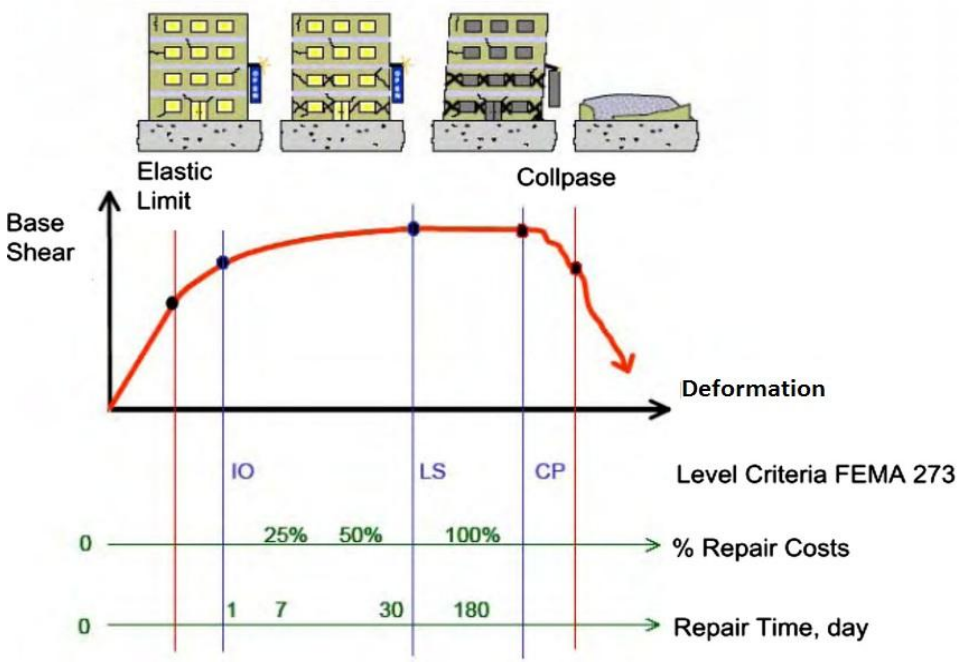

FIGURE 2.7: FEMA 273/356 performance levels

FEMA-356 (2000) and ATC-40 (1996) outline four analytical methods for analysis and design purposes known as Linear Static Procedure (LSP), Linear Dynamic Procedure (LDP), Nonlinear Static Procedure (NSP) and Nonlinear Dynamic Procedure (NDP). In the present study, only nonlinear static pushover analysis is done for the damage assessment of a case study building.

Target displacement and yield mechanism are the two design parameters that are required for calculation of seismic base shear up to specific hazard level and are directly linked with degree and distribution of structural damage, respectively (Goel, S. C. et al., 2010). The whole structure is then pushed to a calculated target displacement to balance the work-energy principle (Zhang, Q. et al., 2017; Goel, S. C. et al., 2010). Nonlinear analysis is then performed to design the frame elements and joints to attain the desired yield mechanism and behaviour. The described procedure is reasonably expedient for multistorey high-rise buildings (Zhang, Q. et al., 2017; Goel, S. C. et al., 2010). Recently PBSD has been a globally known methodology for advanced seismic design in the future (Wei, L. and Qing, 2012; Ning, L., 2012).

2.6 Nonlinear Static Pushover Analysis (PoA)

Nonlinear Dynamic Procedure (NDP) is theoretically real approach for analysis and design of structures (Martino, A. R., 2000; Elnashai, A. S., 2001; Fajfar, P., 2002; Giannopoulos, P. I., 2009; Poluraju, P., Rao, N., 2011; Vijaykumar, A., Babu, D. L. V., 2012). NDP can precisely approximate the seismic demand and seismic capacity of a structure in case of a an EQ. (Jalilkhani et al., 2020). However, it is very complicated and not suitable for every structure as it requires time history of ground shaking and hysteretic behaviour of structural components. For this reason, engineers nowadays prefer nonlinear static pushover analysis.

Pushover analysis (PoA) is a modern and unconventional static nonlinear methodology. Valuable information about the structure like lateral load capacity, formation of hinges, and failure mechanism can easily be extracted using PoA approach (Jalilkhani et al., 2020). PoA is a blend of nonlinear static analysis and seismic response spectrum that makes it a good tool for the evaluation of structures inelastic demand (Ye, L. and Pan, W., 2000). PoA is a simple yet effective tool to monitor the behaviour of a structure beyond the elastic limit (Hakim et al., 2014). PoA is based on the supposition that structure lies in fundamental mode

during a seismic event. In other words, the response of multi-degree-of freedom (MDOF) system can be related to an equivalent single-degree-of-freedom (SDOF) system i.e. response will be dominated by the fundamental mode only and shape of fundamental mode will remain same. Evidently, this is in contrary to the reality but research studies (Martino, A. R., 2000; Fajfar, P., 2002; Themelis, S., 2008) in literature proposed that the two assumptions result in good and reliable forecast for maximum seismic response of MDOF.

PoA was first used by Freemen et al. (1975) in U.S. marine forces project for seismic assessment of a series of 80 buildings. Later, it was used as a relation between seismic ground shaking and building performance. In PoA, the structure is pushed statically upto a pre-defined displacement or force. PoA produces a capacity curve that is basically a graph between roof displacement and base shear as pictured in Figure 2.8. The capacity curve predicts if there is any premature failure or weakness in the structure or how the structure will perform in the plastic range (FEMA-356, 2000; ATC-40, 1996). The main steps of PoA are presented in Figure 2.9.

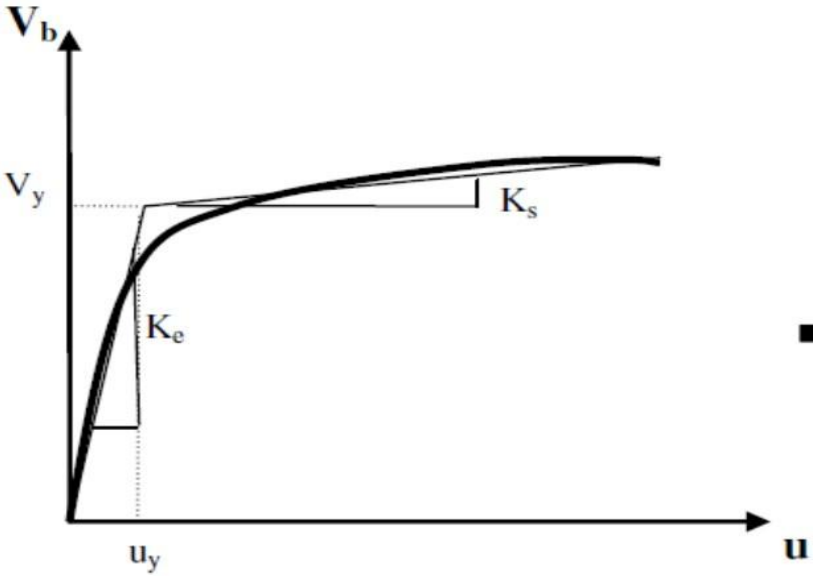

FIGURE 2.8: Capacity curve for MDOF system (Themelis, S., 2008)

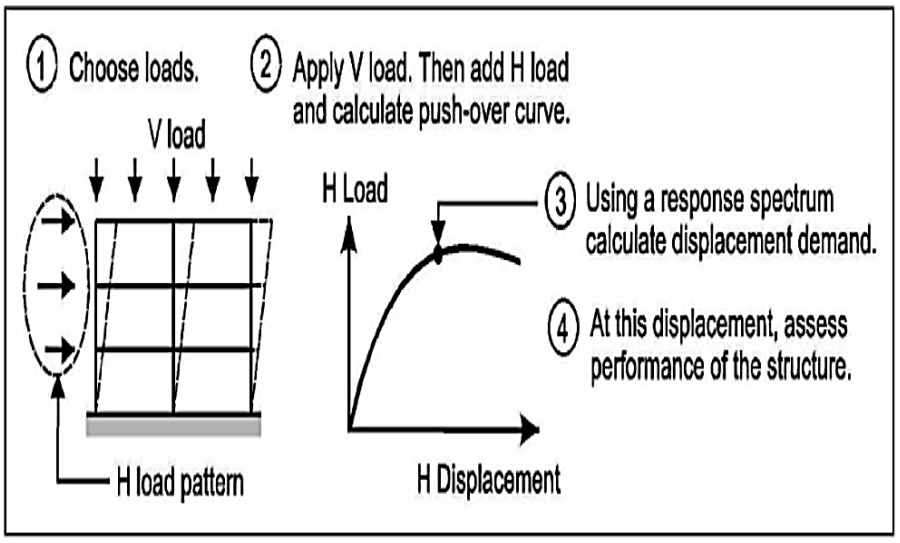

FIGURE 2.9: Main steps for PoA

PoA can be performed by one of the following methods: Capacity Spectrum Method (ATC-40, 1996), Displacement Coefficient Method (FEMA-273, 1997; FEMA-356, 2000) or Displacement Modification Method (FEMA-440, 2005). The most commonly used method is Displacement Coefficient Method which requires the approximation of target displacement (Δt). The target displacement incorporates the inelastic behavior of the structure and is calculated using the equation given below.

$\Delta \mathrm{t} = \mathrm{C}_0 C_1 C_2 C_3 S_a T_e^2 / 4\pi^2 g - - - Equation(2.3)$

Where:

C_0 = Modification factor to incorporate the spectral displacement.

C_1 = Modification factor to account for the ratio of expected inelastic to elastic response displacement

C_2 = Modification factor to represent the effect of hysteresis shape.

C_3 = Modification factor for increased displacement due to P-delta (P-Δ) effect.

S_a = Response spectrum acceleration, g.

T_e = Effective time period, sec.

g = Gravity acceleration

In PoA, response of plastic hinges is assessed by load-deformation curve as depicted in Figure 2.10. The points A, B, C, D, and E on the curve represent the deflected state of hinge. Point A is the unloaded condition and point B is the yield point. The line AB is the elastic response of the hinge. After yielding, the stiffness reduces from point B to C. Point C has resistance equal to nominal strength of the component. The slope of line BC normally ranges from 0% to 10% of the initial slope. Then there is abrupt decrease in lateral load resistance. Point D represents the response at reduced resistance. Point E depicts the total loss of resistance. The line CD relates to the initial failure of element. The line DE is the residual strength of the element. The points between B and C represent the performance of the hinge. The IO, LS and CP correspond to Immediate Occupancy, Life Safety, and Collapse Prevention, respectively. For each limit state (IO, LS, CP), values of different parameters (a, b, c), depending upon component and material type, are given in FEMA-356 (2000) and ATC-40 (1996).

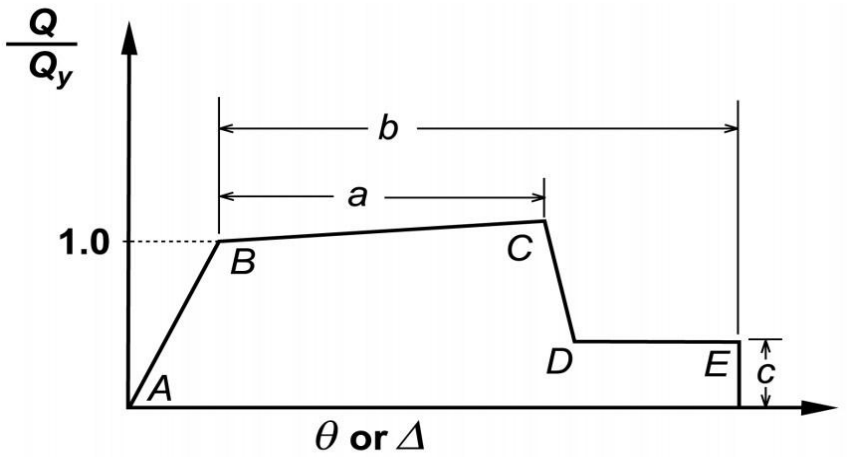

FIGURE 2.10: Force-deformation curve for hinges (FEMA-356, 2000)

2.7 Summary

Different numerical and experimental approaches and techniques adopted by different researchers for earthquake damage assessment of structure have been presented. Earthquake phenomenon, seismic design philosophy, and necessity of seismic damage assessment is described briefly. Effectiveness and limitations of ESA are discussed. PBEE and PBSD have been portrayed. Furthermore, non-linear static PoA is also outlined.

Chapter 3

Modeling and Design of Case Study Building

3.1 Introduction

In the current research study, an effort has been made to explore the performance of a RC frame structure against earthquakes of different intensities in order to evaluate damage assessment and estimate cost and time required for retrofitting. For this purpose, a real-life 7-storied building has been chosen. ESA and PoA have been performed using a commercially available structure software SAP-2000 v15.0.0. Different seismic response parameters like storey shear, storey moment, storey displacement, and storey drift have been computed and compared. Damage has been assessed and cost and time required to recover the damage has also been estimated.

3.2 Description of the Case Study Building

The project is a real life existing mid-rise 7-storey RC frame building located at the heart of the capital of Pakistan, Islamabad. The building has a basement and Ground+5 stories. It is a multi-purpose 40 ft by 40 ft building with commercial

shops and offices having light weight partition walls. The facade of the building consists of light weight curtain walls. Overall height of the under consider building is 75.25 ft and typical height of each storey is 12 ft. The typical architectural plans of the under study building are portrayed in Figures 3.1 and 3.2.

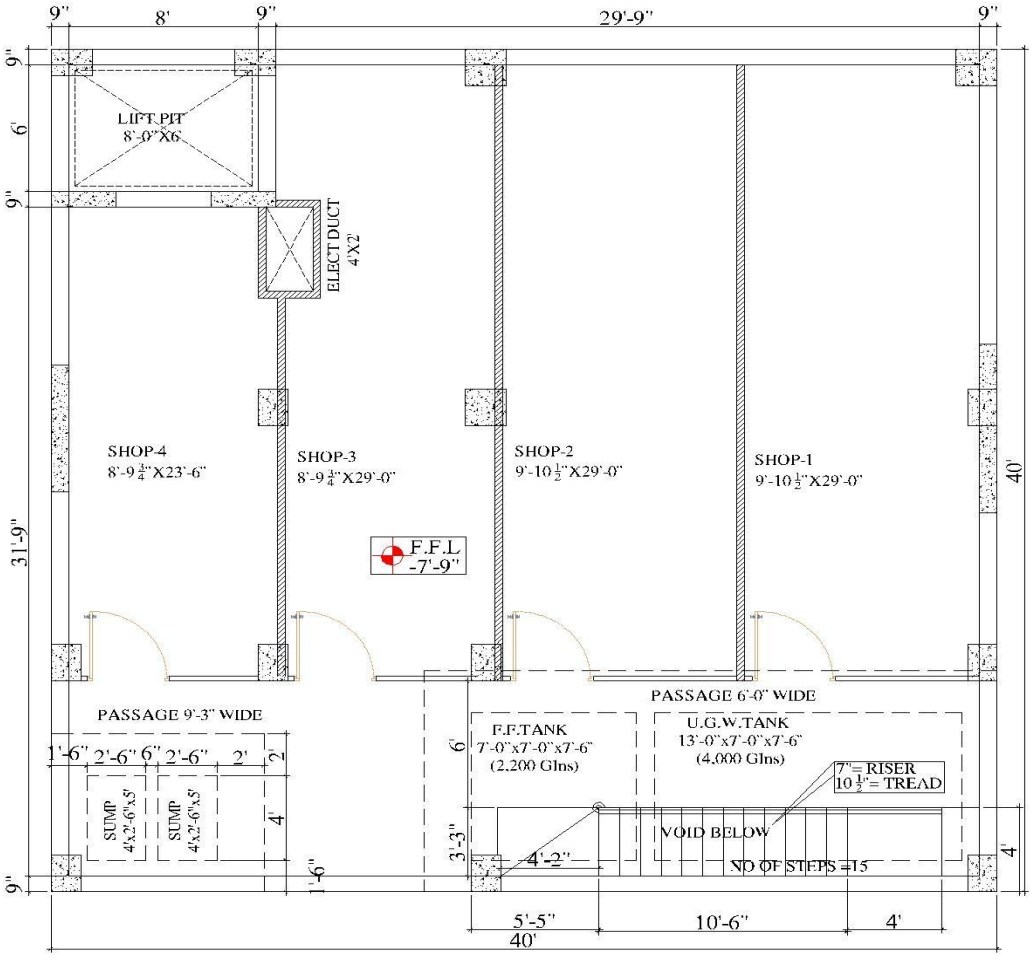

FIGURE 3.1: Typical commercial shops plan

There are 3 and 4 spans in X- and Y-direction, respectively. The grid spacing is 9.125 ft, 9.25 ft, and 21.625 in X-direction and 10.75 ft, 12.25 ft, 9.875 ft, and 7.125 ft in Y-direction. Seismic zone and soil profile type of under consider building, as per UBC (1997) and soil investigation report, are 2B and S_D (stiff soil), respectively. The finite element model (FEM), elevation, and typical framing of the building are depicted in Figures 3.3(a), (b) and 3.4, respectively. The structural system of the building is intermediate moment resisting frame (IMRF) in X-direction and dual system in Y-direction due to presence of shear walls.

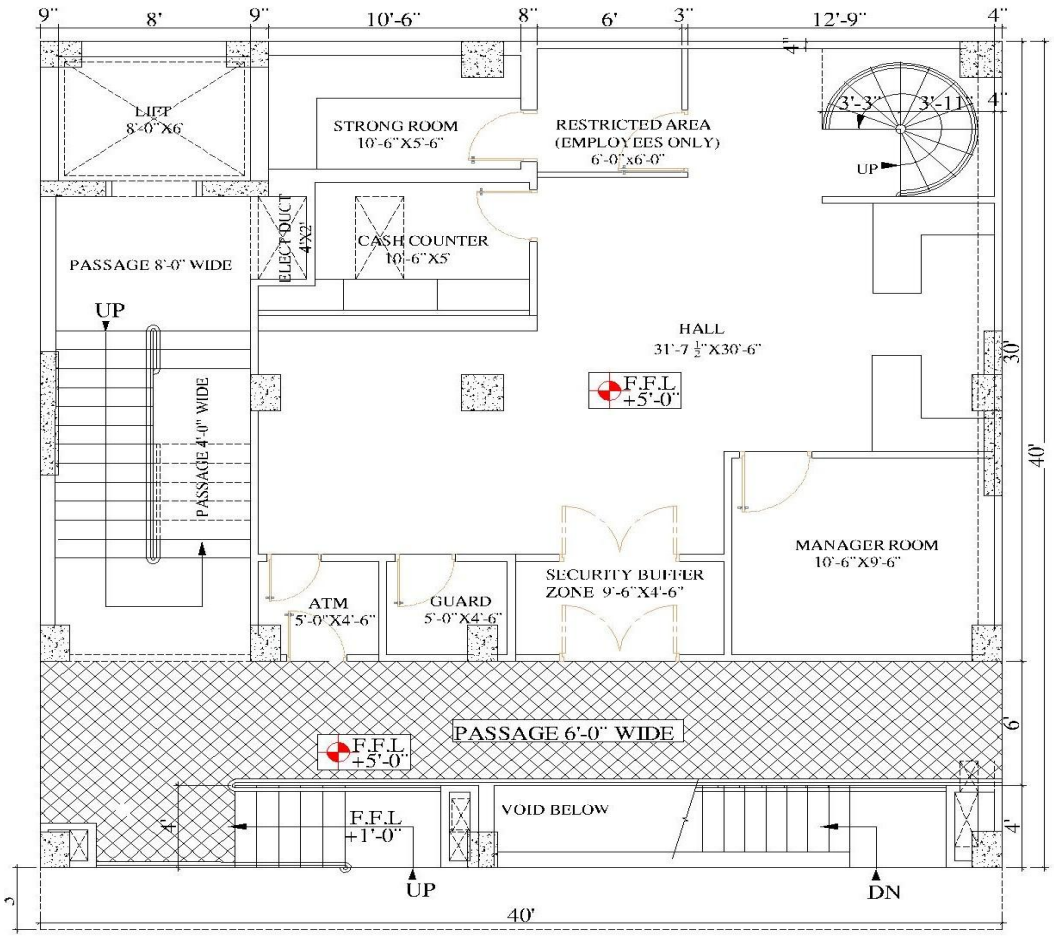

FIGURE 3.2: Typical office floor plan

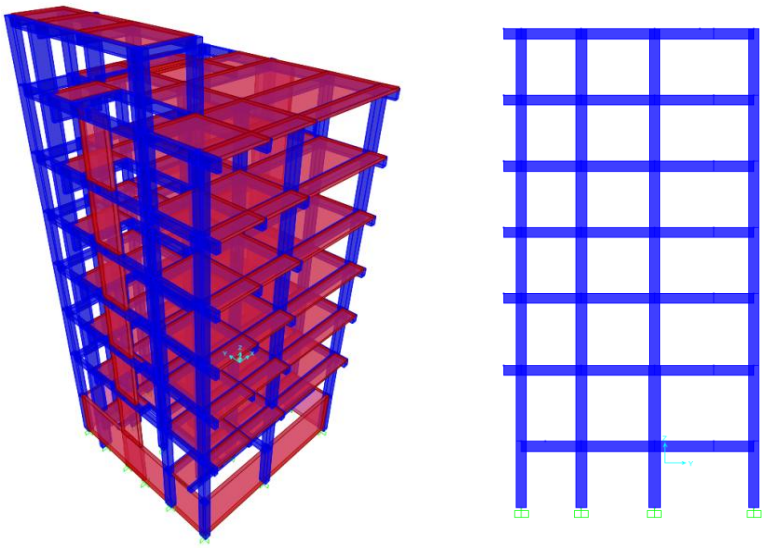

(a) (b)

FIGURE 3.3: (a) FE model of the building (b) Side elevation of the building

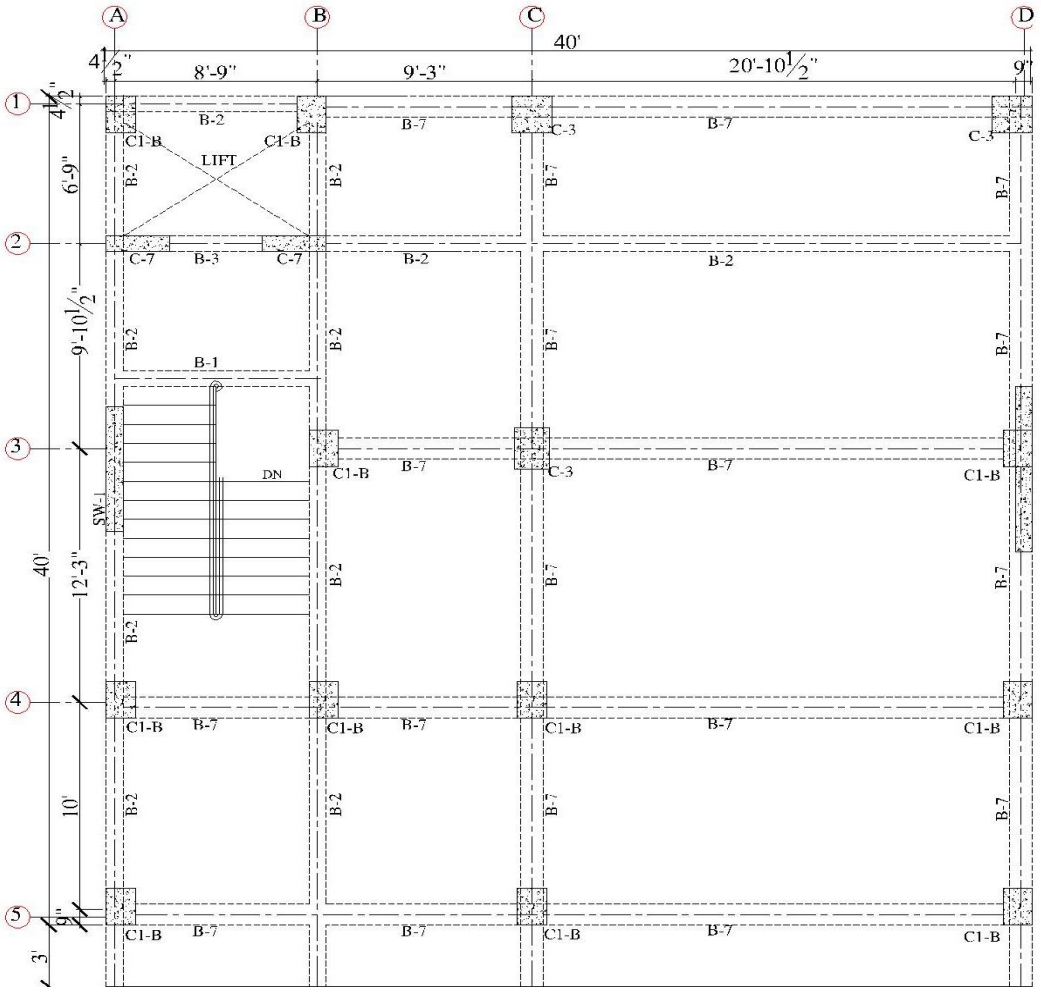

FIGURE 3.4: Typical framing plan of the building

All reinforced concrete (RC) beams and columns are modeled as frame sections while RC slabs and shear walls are modeled as shell elements. Fully rigid connections are used to model joints. Material properties include concrete compressive strength of 3000 psi for slabs and beams and 4000 psi for columns and shear walls to follow the strong-column-weak-beam concept. Rebar strength is taken as 60,000 psi for longitudinal and transverse reinforcement as mentioned in general notes of the structural drawings of case study building. General notes for the case study building is attached as Annexure A at the end of the thesis. Cross-sectional sizes and material properties of the structural elements are taken as per actual structural drawings of the building. Material properties and cross-sectional sizes of the structural elements are shown in Table 3.1 and Table 3.2, respectively. Slab

thickness is taken as 6 inches.

TABLE 3.1: Material properties

Member	fc' (ksi)	fy (ksi)
Slab	3	60
Beam	3	60
Column	4	60

TABLE 3.2: X-sectional details of structural elements

Structural Member	X-sectional size (in x in)	Assigned to floor	Structural Member	X-sectional size (in x in)	Assigned to floor
B1	9 x 15	B, G, 1^{st}, 2^{nd}, 3^{rd}, 4^{th}, 5^{th}	C1A	15 x 21	B, G
B2	9 x 21	B, G, 1^{st}, 2^{nd}, 3^{rd}, 4^{th}, 5^{th}	C1B	15 x 21	B, G,1^{st}, 2^{nd}, 3^{rd}, 4^{th}, 5^{th}
B3	9 x 54	G, 5^{th}	C2	18 x 24	B, G
B4	9 x 66	1^{st}, 2^{nd}, 3^{rd}, 4^{th}	C3	18 x 21	1^{st}, 2^{nd}
B5	9 x 75	B	C4	21 x 21	B, G
B6	12 x 12	B	C5	21 x 18	1^{st}, 2^{nd}
B7	12 x 21	B, G, 1^{st}, 2^{nd}, 3^{rd}, 4^{th}, 5^{th}	C6	21 x 15	3^{rd}, 4^{th}, 5^{th}
			C7	33 x 9	B, G,1^{st}, 2^{nd}, 3^{rd}, 4^{th}, 5^{th}

3.3 Equivalent Static Analysis (ESA)

Equivalent static analysis (ESA) is a simplified lateral force method for seismic assessment and is extensively used for elastic analysis of a structure. In this procedure, effect of dynamic loading is replaced by a static lateral force that is distributed over the total height of the building. The building is free of any type of irregularity. Modal Analysis is first performed to determine the vibration modes of the building. Adequate numbers of modes resulted from linear static force

procedure are considered with the goal that over 90% of mass participation ratio is accomplished. From modal analysis, the modal participation factor for the first mode was found more than 75% i.e. the building is first mode dominant. Thus, the building fulfills the limitation for use of ESA. The dead load consists of self weight of the building, load of 3" finishes and partition walls. Dead and live loads are used as per ASCE-07 (2007). Live load is taken as 60 psf and dead load of 55 psf is taken for all floors. For linear static analysis, static load combinations of UBC (1997) are followed. Mass source is taken from 100% of dead load plus 25% of live load as per BCP (2007) and UBC (1997). For the cracked section model, the gross moment of inertia is decreased to 70% for columns and shear walls and 35% for beams and slabs, as per ACI-318-08 (2008). The fixed supports are utilized to simulate soil and super structure interaction.Value of response modification factor, R, is taken as 5.5 considering moment resisiting frame building. Importance factor value for the building is taken as 1. Seismic coefficients Ca and Cv are taken as 0.28 and 0.40, respectively. The time period (Method B) from code based analysis comes out to be 1.03 sec and 0.59 sec for X- and Y-direction, respectively. This time period is believed to be based on contribution of structural and non-structural members (Williams A., 1997). For seismic performance evaluation, only gravity and in-plane forces are taken into account.

3.4 Preparation of Non-linear Models

Non-linearity in the analytical models can be induced either by distributed plasticity (plastic zone) or concentrated plasticity (plastic hinge). However, plastic hinge approach is mostly preferred as it is simple and easy. Distributed plasticity is best suited for the exploration of the behavior of complex members under combined actions of axial forces, bi-axial moments, and buckling effects. In the present study, plastic hinge approach is adopted. The non-linear models have been prepared by inducing non-linearity at both ends of each beam, and at bottom ends of the bottom storey columns in accordance with the physical admissible plastic hinge mechanism.

3.5 Assignment of Plastic Hinges

In the modern world, most of the RC structures are designed with intention that formation of plastic hinges occur during strong ground motion. Formation of plastic hinges in structural components is of vital importance as it not only incorporates the inelastic behavior of the structural member but also redistributes the moment enhancing the load carrying capacity significantly. Once the member is in inelastic zone and hinge moment capacity is reached, formation of hinges starts and with increase in applied loads, hinges continue to rotate until it reaches the maximum rotation capacity. Further increase in applied load results in failure of the structural component (Marder et al., 2020; Farouk and Khalil, 2020).

In SAP 2000, there are two types of hinge definition: i) default auto hinges and ii) user-defined hinges. Default auto hinges include Axial P, Shear V2, Shear V3, Torsion T, Moment M2, and Moment M3 hinges. These hinges are uncoupled and can be utilized individually. Also, the interacting P-M2-M3 coupled hinge is a default auto hinge type. Default auto hinges are based on geometry of structural member and area of reinforcement resulted from ESA and load combinations including gravity and seismic shears and moments. In user-defined hinges, different parameters and acceptance criteria is defined by the user as per requirement. In user-defined hinges, exact reinforcement resulted from static analysis is to be modeled to get the values of moments and rotations. While in auto hinges, values of positive and negative moments are taken from results of static analysis. Plastic hinges can be assigned at any location through member but are usually assigned to critical and physical admissible locations.

For beams, auto M3 hinges are defined and assigned at both ends of each beam. Definition of hinge in SAP 2000 is pictured in Figure 3.5. It can be noted in the figure that auto hinge type and table for RC beams are selected as per criteria of FEMA-356 (2000), Table 6-7. Acceptance criteria for IO, LS and CP levels as per FEMA-356 (2000) and relationship for displacement controlled parameters, moment and rotation, for a typical hinge is shown in Figure 3.6. It can be noted that the typical hinge shown in Figure 3.6 is taking a positive moment capacity

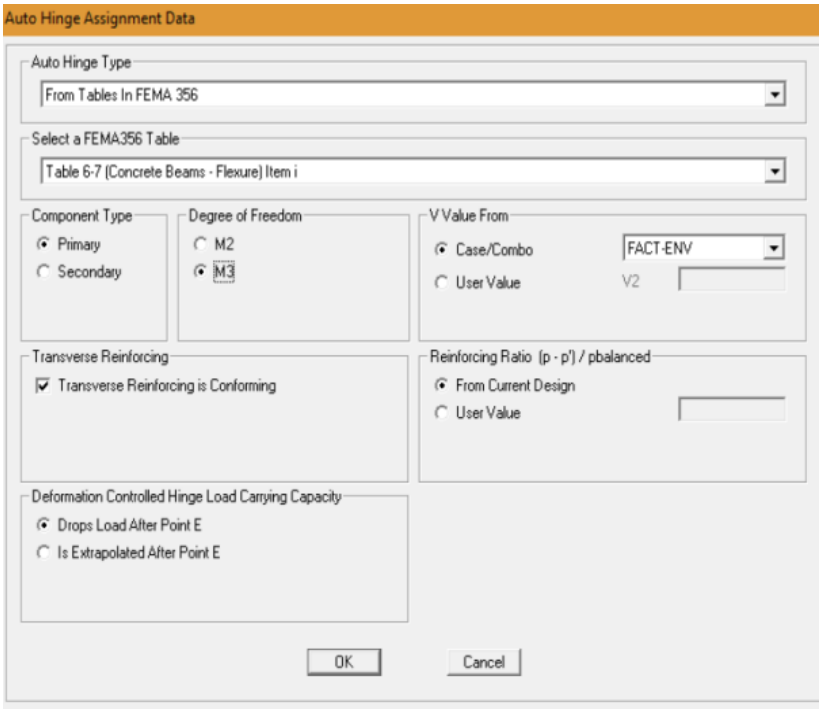

FIGURE 3.5: Auto M3 hinge definition for beams

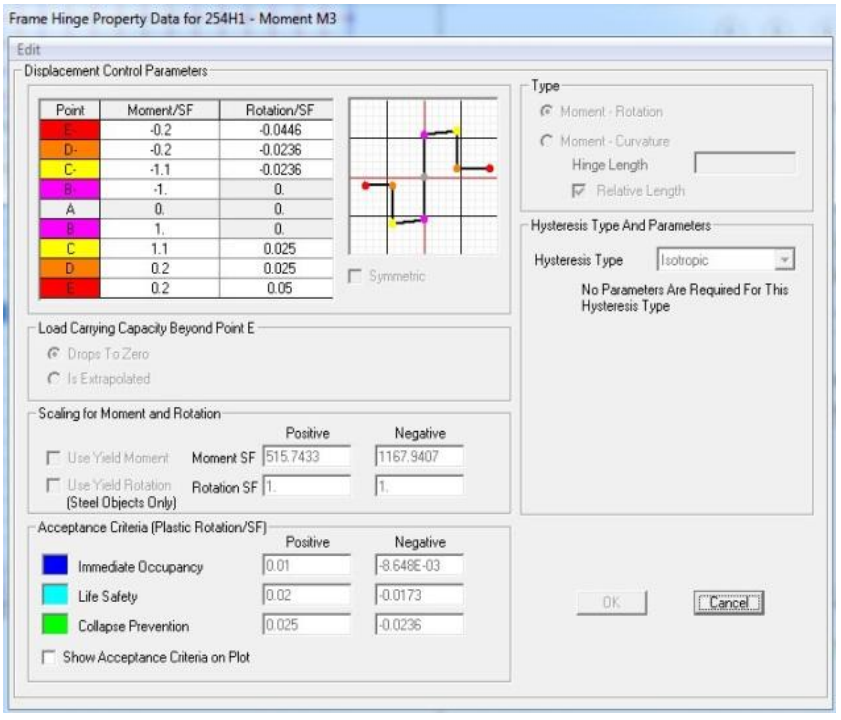

FIGURE 3.6: Auto M3 frame hinge property data

of 516 kip-in and a negative moment capacity of 1168 kip-in. To verify either the hinge is taking the right amount of moment or not, the moment capacity was calculated manually using Equation 3.1. It comes out to be positive moment of 562

kip-in and negative moment of 1280 kip-in which shows the hinge is performing well and taking approximately same amount of moment.

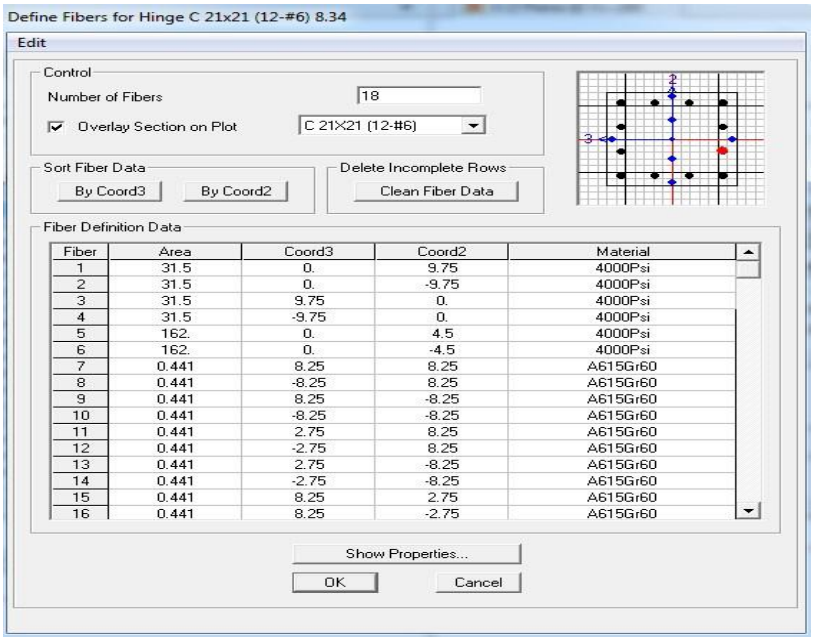

FIGURE 3.7: P-M2-M3 fiber hinge definition for columns

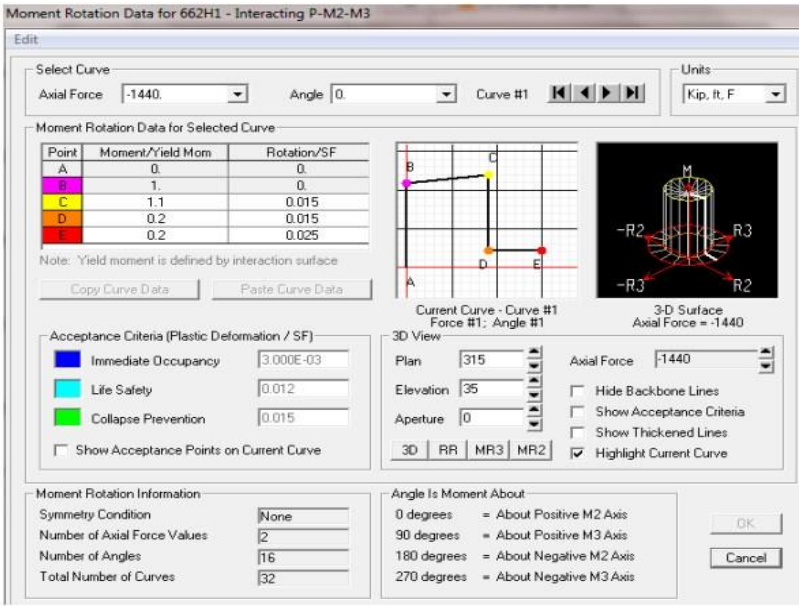

FIGURE 3.8: Interacting P-M2-M3 hinge property data for columns

$$\mathrm{M}=\mathrm{A}_s f_y\left(d-\frac{A_s f_y}{0.85 f_c' 2b}\right) - - - \textit{Equation}(3.1)$$

where:

M = Resulted moment (kip-in)

A_s = Area of steel (in^2)

f_y = Yeild strength of rebar (ksi)

f_c = Crushing strength of concrete (ksi)

d = effective depth of beam (in)

b = beam width (in)

For columns, interacting P-M2-M3 coupled fiber hinges are defined and assigned to the bottom ends of the bottom storey columns. Fiber hinge definition is shown in Figure 3.7. In each fiber hinge, 6 concrete fibers are defined and the number of steel fibers is taken as per the number of steel rebars resulted from ESA. Interacting P-M2-M3 column hinge moment rotation relationship and acceptance criteria for IO, LS and CP levels is shown in Figure 3.8 while moment-curvature curve for column is portrayed in Figure 3.9.

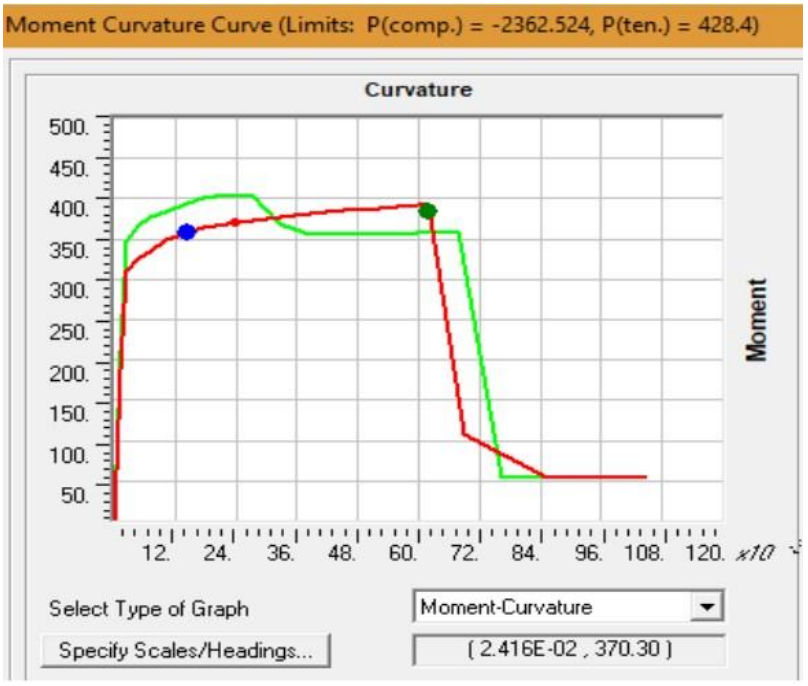

FIGURE 3.9: Moment-curvature relationship for column hinge

Different parameters and acceptance criteria for RC column hinges have been illustrated in FEMA-356 (2000), Table 6-8. As per the Table 6-8, hinge is said to

be in IO, LS, and CP range if the rotation angle is less or equal to 0.005, 0.015, and 0.020 radians, respectively.

3.6 Plastic Hinge Length (l_p)

Seismic performance of a structure is highly influenced by plastic hinge length and must be formulated to fulfill deformation capacity in case of seismic event (Andres et al., 2016). Plastic hinge length should be rational and known for approximating the scope of retrofitting of existing structures as well as seismic design of new structures (Yuan and Wu, 2017; Ren et al., 2020). Plastic hinge length have a critical role in analysis of structures subjected to strong ground motions (Ren et al., 2020). Although plastic hinge length does not affect base shear capacity but has substantial influence on displacement capacity of RC frame structures (Zhao et al., 2011). Different plastic hinge length expressions have been proposed by different researchers as shown in Table 3.3. Upto 30% variation in displacement capacity is observed when different plastic hinge lengths are used (Inel and Ozmen, 2006). Effective plastic hinge length can be determined using formula proposed by Priestley et al. (1996) as expressed below in Equation 3.2 and is also used in guidelines of ATC-32 (1996).

$l_p = 0.08l + 0.15d_b f_y \quad --- Equation(3.2)$

where:

l_p = Plastic hinge length (in)

l = Distance from critical section to contraflexure point (in)

d_b = Dia of rebar (in)

f_y = Yield strength of rebar (ksi)

Alternatively, $l_p = 0.5h$, where h is total depth of the member is the easiest and the simplest expression for plastic hinge length and can be utilized for typical beam and column section (Park and Paulay, 1975). In the current case study, Equation

3.2 has been used for defining the plastic hinge lengths for RC beams and columns. Plastic hinge length for a column, calculated from Equation 3.2, used in definition of P-M2-M3 hinge is shown as an example in Figure 3.10. In Figure 3.10, it must be noted that user defined option is selected for fiber definition and hinge length of 0.695, calculated from Equation 3.2 for a particular column, is entered in hinge length box.

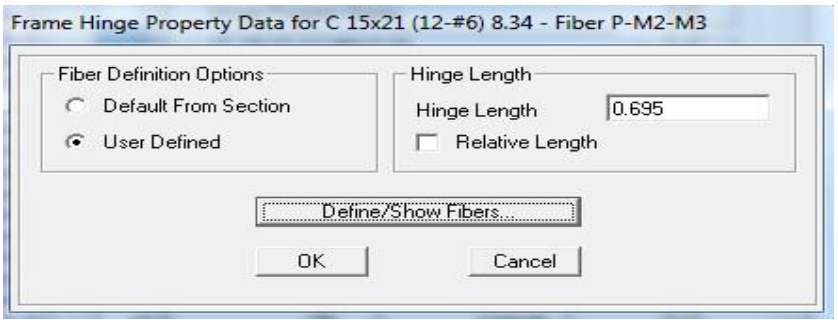

FIGURE 3.10: Hinge length in definition of a column P-M2-M3 fiber hinge

TABLE 3.3: Empirical expressions for plastic hinge length (l_p)

Sr. No.	Proposed by	Plastic Hinge Length Expression (l_p)
1	Barker (1956)	$k(l/d)^{1/4}$ d
2	Sawyer (1964)	0.25d+0.075l
3	Corley (1966)	$0.5d+0.2\sqrt{d(l/d)}$
4	Mattock (1967)	0.5d+0.05l
5	Priestley and Park (1987)	$0.08l+6d_b$
6	Paulay and Priestley (1992)	$0.08l+0.022d_b f_y$
7	Sheihk and Khoury (1993)	1.0h
8	Coleman and Spacone (2001)	G_f^C / [$0.6f_c$ (ϵ_0-ϵc+$0.8f_c$ / E_c)]
9	Panagiotakos and Frandis (2001)	$0.18l+0.021d_b f_y$
10	Bae and Bayrak (2008)	l_p / h = [0.3(p-p_0)+3(As/Ag)-1] (1/h) + 0.25≥0.25

3.7 Push-over Analysis (PoA)

Push-over Analysis (PoA) is a non-linear static analysis procedure as previously explained in Chapter 2. In this procedure, the structure is pushed monotonically with a defined loading pattern until it reaches a predefined target displacement (Δt). This results in push-over curve, also known as or inelastic demand curve, which is basically a graph between base shear and roof displacement as shown in Figure 2.8. Since the case study building is first mode dominant, push-over analysis is preferred to assess seismic performance of the building. In the current case study, push-over analysis has been performed as per guidelines of FEMA-273 (1997) and ATC-40 (1996). The target displacement has been calculated using Equation 2.3. As per ACI-318-08 (2008), structural components are modeled as cracked section for the case study building. Thus, gross moment of inertia is decreased to 70% for columns and shear walls and 35% for beams and slabs. The values of effective time period (Te) with cracked section properties, 1st mode displacement, and modal participation factors are obtained from modal analysis. As the current study is for damage assessment, only 1st mode displacement is considered which is closely related to deformation (rotation) demand. Deformation demand is usually dominated by 1st mode while the higher modes can dominate the force demands as the higher modes have high stiffness. The effective time period from Method B in X- and Y-direction is taken from mode 1 and mode 3 of modal analysis as mass participation in X- and Y-direction is dominant in mode 1 and mode 3, respectively. The Equation 2.3 is for calculating target displacement at DBE. For target displacement at MCE and SLE, spectral accelration is multiplied and devided by 1.5 and 1.4, respectively. Target displacements for each earthquake level (SLE, DBE, MCE) in X- and Y-direction are illustrated in Table 3.4.

Non-linear static gravity load case is first defined as 1.2D+L_s+0.5L. It is a modal load combination and is a specialized type of loading used for pushover analysis. It is a pattern of forces on the joints that is proportional to the product of a specified mode shape times its circular frequency squared times the mass tributary to the joint. Directional effects have been incorporated in the definition of load cases

TABLE 3.4: Target displacements for different EQ levels in X- and Y-direction

Values	X-direction			Y-direction		
	SLE	DBE	MCE	SLE	DBE	MCE
C0	1.5	1.5	1.5	1.5	1.5	1.5
C1	1	1	1	1	1	1
C2	1	1	1	1	1	1
C3	1	1	1	1	1	1
Sa	0.273	0.383	0.574	0.487	0.683	1.024
Time Period (sec)	1.03	1.03	1.03	0.59	0.59	0.59
Target Displacement (in)	4.25	5.96	8.94	2.81	3.49	5.23
Target Displacement (ft)	0.35	0.49	0.74	0.23	0.29	0.43

Push-X and Push-Y as per UBC (1997). Load case Push-X has been defined including 100% load in X-direction plus 30% load in Y-direction. Likewise, load case Push-Y is defined including 100% load in Y-direction and 30% load in X-direction. The load cases Push-X and Push-Y continue from state at end of non-linear gravity case 1.2D+L_s+0.5L. The definition of non-linear load cases Push-X and Push-Y is shown in Figure 3.11. These non-linear load cases have been defined for each level of EQ (SLE, DBE, MCE) with target displacements as shown in Table 3.4.

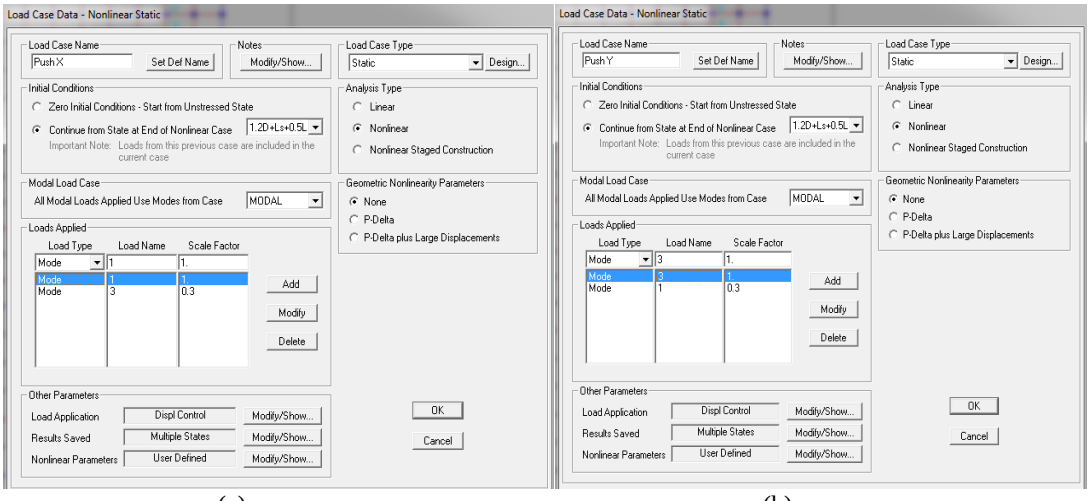

(a) (b)

FIGURE 3.11: Nonlinear load case definition (a) Push-X (b) Push-Y

3.8 Damage Assessment

Seismic damage assessment may be carried out for a number of versatile purposes like seismic design optimization, EQ insurance considerations, EQ hazard reduction etc. Many researchers and investigators have proposed different methodologies for prediction of structural damage in case of an EQ. Although quantification of seismic damage that is likely to happen to a structure is a probabilistic problem, many researchers have come up with deterministic approaches that have been proved to be useful tool for damage assessment. These deterministic approaches involve engineering demand parameters (EDPs) such as stress, strain, displacement, curvature, rotation, base shear, strength, stiffness, and energy dissipated. A damage is a combination of EDPs representing different modes of failure resulting a numeric value, which ranges between zero to unity (Kappos, 1997). A list of DIs along with engineering parameter is shown in Tables 3.5 and 3.6. Also, several researchers have proposed their own range of DI with respect to different EDPs to define the damage state of the structure or a component of a structure as represented in Table 3.7.

When a seismic event happens, deformation occurs. Deformation starts from cracking and leads to spalling, crushing, bending or buckling of the component depending upon the seismic and structure response parameters. Cracks in a RC member are not only inevitable, but actually necessary for reinforcement to be effective. So, crack width is another widely used engineering parameter for assessing the seismic damage and classifying the damage states. Definition of crack width proposed by different researchers is given in the following paragraphs.

Gergely and Lutz (1968) proposed the formulation of crack width based on the maximum moments in case of a seismic event. The formulation is valid only upto the yield point of steel. However, the same expression can be used for moments beyond the yield point of steel. In such case, stress in steel is computed by multiplying strain in steel with its initial modulus of elasticity. The expression is shown below in Equation 3.3.

TABLE 3.5: Summary of DIs with their parameters (Zameeruddin and Sangle, 2016)

Sr. #	Proposed by	Description	Formulation
A	Vibration response-based DIs		
1	Local DIs		
a	Newmark and Rosenblueth (1971)	DI is a function of rotation (θ)	$\mu r(\theta) = \frac{\theta m}{\theta y} = 1 + [\frac{\theta m - \theta y}{\theta y}]$
b	Banon et al. (1981)	DI is a function of curvature (ϕ)	μr (ϕ) = $\frac{\phi m}{\phi y}$ =1+[($\frac{\phi m - \phi y}{\phi y}$]
c	Park (1986)	DI is a function of member displacement (δ)	μr (δ)=$\frac{\delta m}{\delta y}$ =1+[$\frac{\delta m - \delta y}{\delta y}$]
d	Lybas and Sozen (1977)	DI is the ratio of initial to maximum elastic stiffness	DI=$\frac{Ko}{Km}$
e	Banon et al. (1981)	Flexure Damage Ratio (FDR) is defined as stiffness degradation	DI=$\frac{Mu\phi m}{Mm\phi u}$
f	Roufaiel and Meyer (1987)	Modified FDR (MFDR) is defined as increment in ductility before and after a failure	DI=[$\frac{\theta m}{Mm}$-$\frac{\theta y}{My}$]/[$\frac{\theta u}{Mu}$-$\frac{\theta y}{My}$]
2	Cumulative DIs		
g	Banon and Veneziano (1982)	Damage Index is the normalized cumulative rotation	DI=[($\Sigma_{i=1}^{m}$ ϕm- ϕy)/ϕu]
h	Stephens and Yao (1987)	Damage Index is the cumulative displacement ductility	DI=$\Sigma_{i=1}^{n}$ [Δd/Δdf]$^{(1-br)}$ b = 0.77 (recommended)
i	Jiang and Iwan (1988)	Forced-based DI accounting the effects of combining cycles with various amplitudes	DI=$\Sigma_{i=1}^{n}$ [n$_i\mu_i^2$/C]

$$W_{max}=0.076\beta f_s \sqrt[3]{d_c A_e} \times 10^{(-3)}(inches) - - - Equation(3.3)$$

Where:

Wmax = maximum crack width

β = ratio of distances between neutral axis to tension face and neutral axis to reinforcing steel centroid

f_s = stress in steel

TABLE 3.6: Summary of DIs with their parameters (Zameeruddin and Sangle, 2016)

Sr. #	Proposed by	Description	Formulation
A	Vibration response-based DIs		
1	Combined DIs		
a	Banon and Veneziano (1982)	DI is a linear combination of maximum displacement, failure displacements, and hysteretic energy dissipation	DI=$\sqrt{\frac{d_m}{d_y-1}^{(2)} + \frac{2E_h}{F_y d_y}^{(0.38)}}$
b	Park and Ang (1985)	DI is a linear combination of maximum plastic displacement and dissipated energy	DI=$\frac{d_m}{d_u} + \beta_e \left[\int \mathrm{dE}/\mathrm{F}_y d_u\right]$
c	Niu and Ren (1996)	Similar t Park and Ang (1985) DI but with different parameters	DI=$\frac{\theta_m}{\theta_u} + \alpha \left[\frac{E}{E_u}\right]^{\beta}$
2	Global DIs		
d	Roufaiel and Mayer (1987)	Strength-based global DIs	DI= GDP$\frac{(dm-dy)}{(du-dy)}$
e	Park and Ang (1985)	DI is defined as hysteretic energy weighted average	$\mathrm{D}_{storey} = (\Sigma_{i=1}^{n} D_i E_i / \Sigma_{i=1}^{n} E_i)$ $\mathrm{D}_{global} = \Sigma_{s,i=1}^{N} D_{s,i} E_{s,i} / \Sigma_{s,i=1}^{N} E_{,i}$
f	Bracci (1989)	DI is defined as gravity load weighted average	$\mathrm{D}_{storey} = \Sigma_{i=1}^{N} W_i D_i^{(b+1)} / \Sigma_{i=1}^{N} W_i D_i^{b}$ $\mathrm{D}_{global} = \Sigma_{s,i=1}^{N} W_{s,i} D_{s,i} / \Sigma_{s,i=1}^{N} W_{s,i} D_{s,i}$
B	Strength parameter-based DI		
g	Ghobarah et al. (1999)	DI shows the percentage variation in the stiffness of a structure	DI=1-$\frac{K_{final}}{K_{initial}}$

d_c = distance between rebar centroid and extreme tension fiber

A_e = effective area of concrete

Frosch (1999) proposed formulation of crack width based on strain in reinforcing steel as shown in Equation 3.4. In this equation, w, s, and d* represent maximum crack width, steel strain and controlling cover distance, respectively. The controlling cover distance is further computed by the relationship given below.

TABLE 3.7: Damage index range for different damage states

Sr. #	Damage State	Damage Index (DI)
1	Ghobarah et al. (1999)	Parameter: Stiffness Index
	None or Minor	0.00 - 0.15
	Moderate (reparable)	0.15 - 0.30
	Extensive (irrepairable)	0.30 - 0.80
	Collapse	> 0.80
2	Kostinakis et al. (2013)	Parameter: Angle of incidence / curvature
	Slight	< 0.10
	Minor	0.10 - 0.25
	Moderate (repairable)	0.25 - 0.40
	Severe (irrepairable)	0.40 - 1
	Collapse	> 1
3	Tabeshpour et al. (2004)	Parameter: Storey drift
	Slight	< 0.10
	Minor	0.10 - 0.25
	Moderate (repairable)	0.25 - 0.40
	Severe (irrepairable)	0.40 - 1
	Collapse	> 1
4	Sengupta (2014)	Parameter: Drift ratio
	Minor	< 0.10
	Low	0.10 - 0.40
	Moderate	0.40 - 0.75
	Severe	> 0.75
5	Komeili et al. (2012)	Parameter: Drift limit (%)
	Minor	0.10 - 0.20
	Moderate	0.20 - 0.50
	severe	0.50 - 1.0
	Collapse	> 1.0

In this relation, dc is clear cover and s is the distance between two aneighboring reinforcement rebars. In this current case study, Equation 3.4 has been used for the computation of crack width. In this study, a constant value of 100 mm is used as the controling cover distance (d*) to elimitate the effect of variations of the reinforcement arrangement.

$w=2\ \varepsilon_s\ d^* - - - \ Equation(3.4)$

$d^* = \sqrt{d_c^2 + [\frac{s}{2}]^2}$

Crack width has been linked with damage state by many researchers as shown in Table 3.8. However, Erduran and Yakut (2004) criteria has been adopted for the current case study.

TABLE 3.8: Crack width, damage state and damage description

Sr. #	Crack Width (mm)	Damage State	Damage Description
1	Sinha and Shiradhonkar (2012)		
	< 0.1	Slight	Very fine cracks
	0.1 - 0.2	Light	Visible cracks
	0.2 - 0.5	Moderate	Large cracks and some spalling of concrete cover
	0.5 - 3	Extensive	Spalling of concrete cover and cracks in core concrete
	> 3 mm	Collapse	Crushing of core concrete
2	Maeda et al. (2004)		
	< 0.2	Minor	Hairline cracks
	0.2 - 1	Light	Noticeable cracks
	1 - 2	Moderate	Heavy cracks with some spalling of concrete
	> 2	Severe	Reinforcing rebars exposed
3	Erduran and Yakut (2004)		
	< 0.2	Minor	Very fine/hairline cracks (0 - 5% damage)
	0.2 - 1.0	Light	Visible cracks (5 - 10 % damage)
	1.0 - 2.0	Moderate	Visible Cracks and some spalling of outer layer (10 - 50 % damage)

For columns, values of strains are taken directly from the SAP-2000 results for fiber hinges as illustrated in Figure 3.12. Maximum value of strain is used to determine crack width in columns using Frosch (1999) equation. As for beams, strain is calculated using section designer in SAP-2000 as shown in Figure 3.13. First, beams were drawn in section designer as per cross-sectional dimensions and

area of steel. Value of moments at the location of hinges were noted from pushover analysis. The value of strain against that moment was then taken fom moment-curvature plot obtained from section designer. Validity of strain was cross checked to ensure the correct results. Value of nominal moment capacity from manual calculation for given cross section and reinforcement, and the value of moment at the loaction of the hinge were found approximately equal as discussed in section 3.5. As auto hinge gives hinge rotation only beyond the yeild point (point B), it was also cross checked. From section designer results, the difference between rotations at design moment and yeild moment was nearly the same as rotation taken by the hinge. These two checks enable us to believe that hinge results and section designer results are valid and can be used for further estimation of crack width. The minor differences may be due to the difference of area of steel required and provided.

Frame Fiber Hinge States 02 - Individual Fibers

File View Format-Filter-Sort Select Options

Units: As Noted — Frame Fiber Hinge States 02 - Individual Fibers

	Frame Text	OutputCase Text	CaseType Text	StepType Text	AssignHinge Text	GenHinge Text	FiberNum Unitless	FiberStress Kip/in2	FiberStrain Unitless
▶	3	Push X	NonStatic	Max	5x21 (12-#6) 8	3H1	1	0.4402	0.00193
	3	Push X	NonStatic	Max	5x21 (12-#6) 8	3H1	2	-0.254	-0.000071
	3	Push X	NonStatic	Max	5x21 (12-#6) 8	3H1	3	0.4407	0.000404
	3	Push X	NonStatic	Max	5x21 (12-#6) 8	3H1	4	0.472	0.000138
	3	Push X	NonStatic	Max	5x21 (12-#6) 8	3H1	5	0.474	0.001037
	3	Push X	NonStatic	Max	5x21 (12-#6) 8	3H1	6	-0.3901	-0.000109
	3	Push X	NonStatic	Max	5x21 (12-#6) 8	3H1	7	51.5638	0.001778
	3	Push X	NonStatic	Max	5x21 (12-#6) 8	3H1	8	45.5689	0.001571
	3	Push X	NonStatic	Max	5x21 (12-#6) 8	3H1	9	-2.1993	-0.000076
	3	Push X	NonStatic	Max	5x21 (12-#6) 8	3H1	10	-2.5604	-0.000088
	3	Push X	NonStatic	Max	5x21 (12-#6) 8	3H1	11	49.5655	0.001709
	3	Push X	NonStatic	Max	5x21 (12-#6) 8	3H1	12	47.5672	0.00164
	3	Push X	NonStatic	Max	5x21 (12-#6) 8	3H1	13	-2.3197	-0.00008
	3	Push X	NonStatic	Max	5x21 (12-#6) 8	3H1	14	-2.44	-0.000084
	3	Push X	NonStatic	Max	5x21 (12-#6) 8	3H1	15	24.4233	0.000842
	3	Push X	NonStatic	Max	5x21 (12-#6) 8	3H1	16	18.4284	0.000635
	3	Push X	NonStatic	Max	5x21 (12-#6) 8	3H1	17	-2.7172	-0.000094
	3	Push X	NonStatic	Max	5x21 (12-#6) 8	3H1	18	-3.7188	-0.000128
	3	Push X	NonStatic	Min	5x21 (12-#6) 8	3H1	1	-0.7596	-0.000213
	3	Push X	NonStatic	Min	5x21 (12-#6) 8	3H1	2	-3.4929	-0.001388
	3	Push X	NonStatic	Min	5x21 (12-#6) 8	3H1	3	-0.4782	-0.000134
	3	Push X	NonStatic	Min	5x21 (12-#6) 8	3H1	4	-0.5542	-0.000155

Record: 1 of 564 Add Tables... Done

FIGURE 3.12: SAP results for individual fiber hinges

FIGURE 3.13: Calculation of strain in beams from SAP-2000 section designer

A building needs to be restored to pre-earthquake condition in terms of strength and stiffness to be functional and safe for inhibitants. It can be done by applying retrofit or repair techniques. In the former, system is upgrated by adding a new element to increase the strength and stiffnesss. This includes adding shear walls, braced frames, buttresses etc. The later includes the strengthing of damaged structural members without adding a new element to the system. It includes epoxy injection, chiken wire mesh, CFRP sheets, and CFRP strips etc. Guidelines for these techniques are outlined in detail in FEMA-356 (2000) and ATC-40 (1996) documents. In the present research project, use of chiken wire mesh, epoxy injection, and CFRP sheets is recommended. The recommendation is based on visit of local offices and exploration of websites like Imporient Group of Companies, Sika Pakistan, Spitpaslode and Hilti Pakistan. Composite unit rates (cost of material+labour+scaffolding) of these materials are taken from local market survay. As there is no research in available literature that propose a relationship between any seismic engineering parameter (stress, strain, hinge rotation, base shear, roof displacement, storey drift etc) and number of cracks occurred in structural component of a building, number of cracks occurred are supposed to be 2, 4, and 6 for negligible, light, and moderate damage state, respectively. Repair remedy adopted

for different damage states along with assumed number of cracks and unit rate of repair technique is shown in Table 3.9.

TABLE 3.9: Repair technique and unit rate for different damage states

Damage State	Repair Technique	No. of cracks assumed	Composite Unit Rate (PKR)
Minor	Chiseling, chipping off plaster and chicken wire mesh	2	150/sft
Light	Low viscosity epoxy injection	4	1000/ft
Moderate	Low viscosity epoxy injection + CFPR wrap	6	1000/ft + 1000/sft

Epoxy injection is widely used and recommended procedure for restoring structural integrity. Low viscosity epoxy injection is used to fill and seal cracks. It not only forms an effective barrier against water infiltration of corrision promoting elements, but also bonds the concrete sections together (ACI Committee E706, 2009). Epoxy injection is very technical work and requires skill and care in executing it. First weak area around crack is chipped off. Crack surface is cleaned with wire brush to make it free of any dust or dirt. Inlet and outlet injection nozzles are fixed on the prepared crack surface and the remaining crack surface is sealed with epoxy adhesive to make the crack leakage free. Epoxy injection is initiated after at least 24 hours of nozzles fixing. Then epoxy is injected via injection pump until it seeps out of the outlet nozzle. Nozzles are corked and the injected cracks are left to cure for 24 hours. Crack length is determined from the x-sectional dimentions of the component. Cost of epoxy injection is then obtained from the product of crack length, number of cracks, and unit price.

Carbon fiber reinforced polymer (CFRP) wrap is an extremely strong and light-weight plastic which contains cabon fibers. It is used to restore initial elastic stiffness, and increase the flexural and shear load capacity of structural components as well as ductilty of columns (Lombard et al., 2000). It is available in ready-to-use form and its application is very easy and simple. The surface, on which CFRP wrap is to be applied, is grinded and made dust free as it needs a good and uniform concrete bonding surface. The surface of application is primed with epoxy with

the help of a roller. The CFRP wrap is cut as per desired length and epoxy is applied on the wrap as well. The CFRP wrap is then applied on the surface and pressed hard to remove any voids and gaps with the help of a special roller. Cost is calculated by multiplying area of CFRP wrap with unit price of CFRP

3.9 Summary

The core objective of the current case study is to evaluate the seismic performance and damage assessment of a building at different intensities of EQ. For this, a realistic 7 storey building has been chosen as case study building. Geometrical, architectural and structural details of the building have been described as well as properties of material, and frame and area elements. Linear ESA and non-linear PoA have been performed to accomplish the said objective. All the parameters required for carrying out the linear and non-linear analysis are explained. Non-linearity has been induced by assigning plastic hinges at suitable locations of the building. Target displacement has been computed for different intensities of EQ as per provisions of FEMA-356 (2000). Push-X and Push-Y load cases have been defined to carry out non-linear analysis in X- and Y-directions, respectively. Purposes and techniques of damage assessment have been described. Methodology and criteria adopted for the current study have been explained. Repair technique for different damage states is recommended based on local market survey. Details of recommended repair technique for different damage states have been briefly explained. Response of different seismic parameters i.e. storey shear, overturning moment, displacement, and drift, and results of damage assessment in terms of cost and time at different levels of EQ have been presented in the proceeding chapter.

Chapter 4

Results and Discussion

4.1 Introduction

In the current study a reslistic 7 story building is modeled and analyzed using static linear and static non-linear procedures. Globally recognized CSI integrated software for structural analysis and design SAP2000 v15.0.0 has been used to perform ESA and PoA. Based on results of analysis, different seismic response parameters like storey shear force, storey over-turning moment, storey displacement, and storey drift have been computed and compared for different levels of EQ i.e. SLE, DBE and MCE. Damage assessment is done by classifying structural members into different damage states i.e. minor, light and moderate. Furthermore, cost and time required for repair have also been estimated at each EQ level. In the following sections these parameters are disscussed one by one in detail.

4.1.1 Center of Mass and Center of Rigidity

It must be noted that there is significant difference between locations of center of mass (CoM) and center of rigidity (CoR) due to presence of shear wall and massive and closely spaced columns towards the right half of the case study building. CoM is the point where whole mass of the storey/building acts and can be supported

under gravitational conditions. CoR is defined as the point where stiffness of storey/building acts. Horizontal structural members (slabs and beams) majorly contribute towards mass while vertical structural components (columns and shear walls) contribute towards stiffness of the building. The distance between CoM and CoR is known as eccentricity which leads to the torsional moments in the building. It is ideal for a building to have CoM and CoR at the same point and better if the difference between them is minimum (Georgoussis, 2020). A number of advantages can be achieved in analysis and design if there is minimum to none difference between CoM and CoR like more stability and safety, less drift, less torsional moments, optimal cross sectional sizes, economization of structural cost, enhanced seismic performance etc. CoM and CoR for the under consider building are presented in Table 4.1 and are visually portrayed in Figure 4.1.

TABLE 4.1: Center of mass and center of rigidity for case study building

		Center of Mass (ft)		Center of Rigidity (ft)	
Floor	Diaphargm Assigned	X	Y	X	Y
Roof	D1	23.55	25.89	22.72	27.27
5th	D1	21.70	22.26	21.95	27.37
4th	D1	21.66	22.19	21.11	27.51
3rd	D1	21.61	22.11	20.11	27.68
2nd	D1	21.56	22.07	18.81	27.68
1st	D1	21.77	22.52	17.26	28.05
Ground	D1	20.26	26.77	19.55	32.99

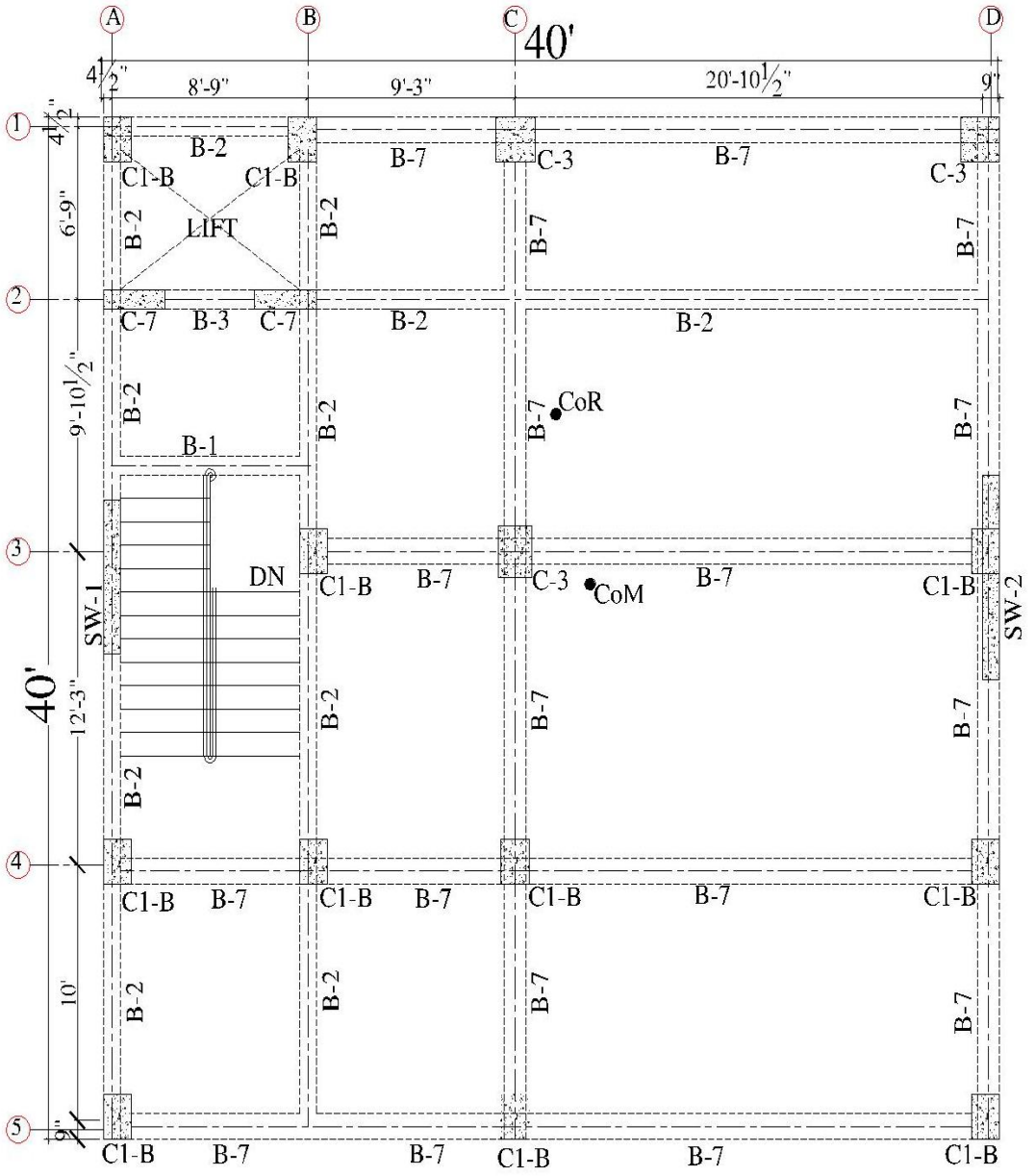

FIGURE 4.1: Center of mass and center of rigidity for case study building

4.2 Seismic Response Parameters

4.2.1 Storey Shear

The lateral force experienced by the building at each storey level resulted by seismic action is called storey shear. This lateral force is distributed over the height of the building and varies from level to level dpending upon stiffness and mass at each level. The cumulative sum of these forces is equal to the force

experienced by the building at the base known as base shear. The storey shear is maximum and equal to base shear at the bottom most storey, decreases gradually over the height and is minimum at the top storey. A comparison of storey shear at different EQ levels for linear static load cases (EX and EY) and non-linear static load cases (Push-X and Push-Y) is presented. Storey shear against different EQ levels is depicted in Figures 4.2a and 4.2b for X- and Y-directions, respectively. A comparison of storey shear at ground floor (level 0) for respective earthquake levels is made which gives the following results. The values and pattern of storey shear against linear static load cases EX and EY are same for all EQ levels. The reason for this is that building is almost symmetric in both plan and elevation. However, storey shear has increased upto 14.84% in Y-direction as compared to that of X-direction in case of PoA. This is because the building has less time period and more stiffness in Y-direction due to shear walls. In case of non-linear load case Push-X, storey shear has inceased 12.49% and 27.33% for DBE and MCE with respect to SLE. While in case of Push-Y, an increase of 13.09% and 39.90% is found for DBE and MCE with respect to SLE. The more the EQ intensity, the more is the base shear that eventually leads to the increase in storey shear. Percentage increase in storey shear for PoA at DBE and MCE as compared to that of SLE is shown in Table 4.2.

TABLE 4.2: Percentage increase in storey shear at DBE and MCE w.r.t. SLE

	Storey Shear at	
Load Case	DBE	MCE
Push-X	12.49%	27.33%
Push-Y	13.09%	39.90%

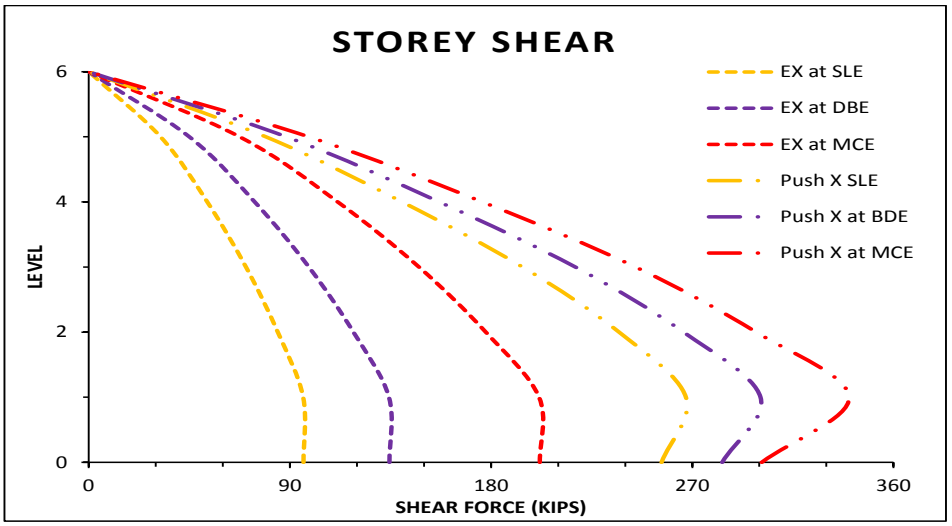

a: Storey Shear in X-direction

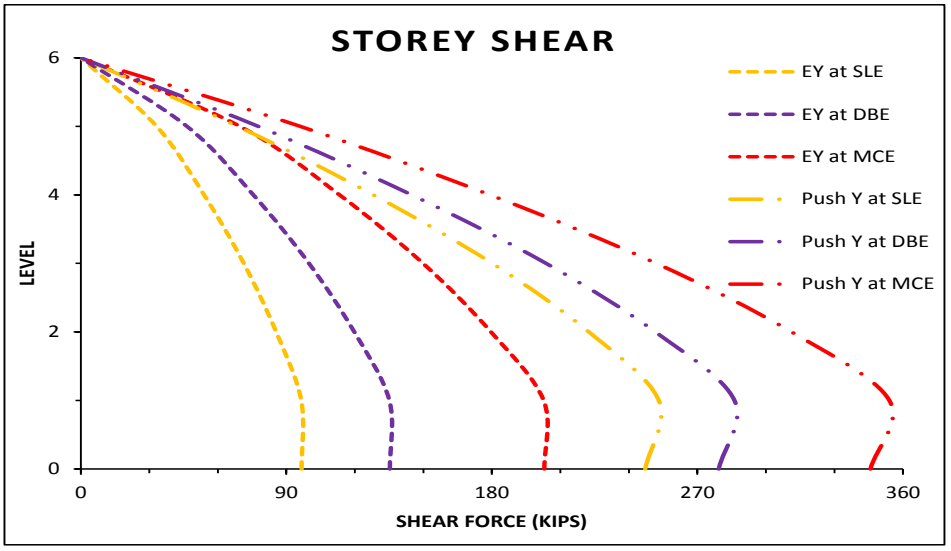

b: Storey Shear in Y-direction

FIGURE 4.2: (a) Storey shear in X-direction (b) Storey shear in Y-direction

4.2.2 Storey Over-turning Moment

The moment that tends to overturn the building at the base is known as over-turning moment and is the product of lateral force and the moment arm upto the specific level. Storey over-turning moment is maximum at the lower most storey and decrease over height as the moment arm decreases. Graphical presentation of storey moment at different EQ levels is pictured in Figures 4.3a and 4.3b for X- and Y-directions, respectively. A comparison of storey moment at ground floor

(level 0) for respective earthquake levels is made which gives the following results. Decrease in overturning moment is observed in Y-direction as compared to that of X-direction for both linear (EX and EY) and nonlinear (Push-X and Push-Y) load cases. A decrease of 12.01% and 3.31% in story moment is calculated for linear and nonlinear load cases, respectively.

TABLE 4.3: Percentage increase in storey over-turning moment at DBE and MCE w.r.t. SLE

	Storey Over-turning Moment at	
Load Case	DBE	MCE
Push-X	24.22%	66.46%
Push-Y	31.31%	86.83%

However, there has been a considerable increase in storey moment for non-linear load cases Push-X and Push-Y. In X-direction, storey moment is increased 24.22% and 66.46% in case of DBE and MCE, respectively as compared to that of SLE. In Y-direction, an increase of 31.31% and 86.83% has been noticed for DBE and MCE in comparison to SLE. As the intensity of a seismic event increases, lateral force distribution at each level also increases and thus the storey over-turning moment. The more increase in storey moment in case of Push-Y is because of shear wall in Y-direction. Percentage increase in storey over-turning moment for PoA at DBE and MCE as compared to that of SLE is shown in Table 4.3.

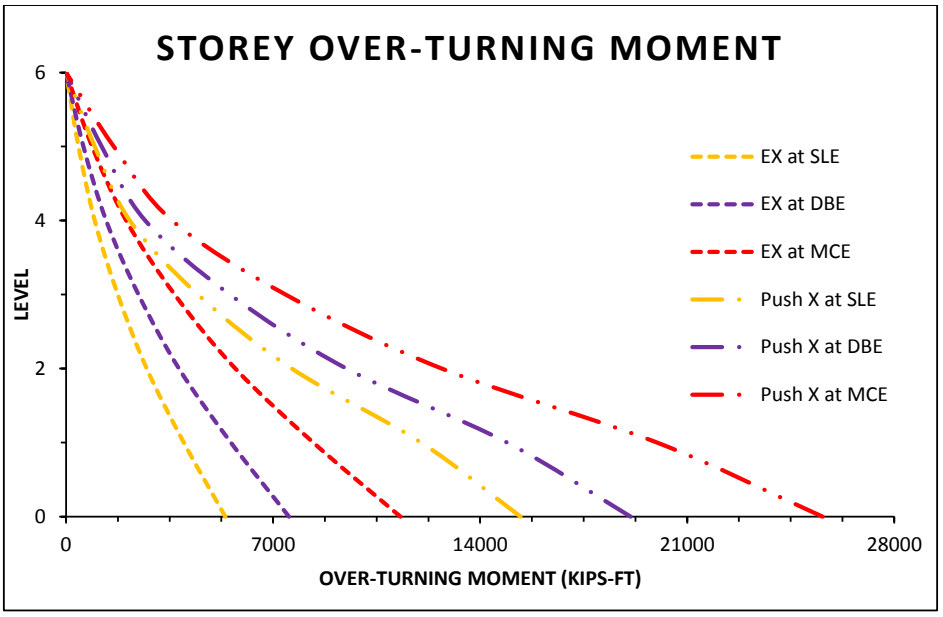

a: Storey Over-turning Moment in X-direction

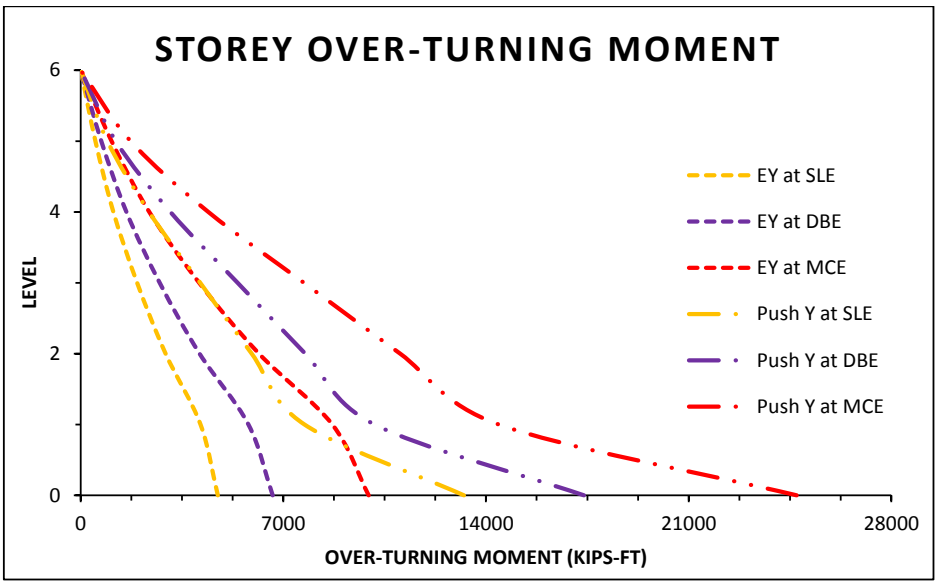

b: Storey Over-turning Moment in Y-direction

FIGURE 4.3: (a) Storey over-turning moment in X-direction (b) Storey over-turning moment in Y-direction

4.2.3 Storey Displacement

Lateral displacement of a storey in comparison to the base is defined as storey displacement. Storey displacement follows the pattern of a SDoF system. As the base is fixed and there is no movement or rotation, storey displacement is zero

at the base, increases as height increases and is maximum at the top. Storey displacement at different EQ levels is portrayed in Figures 4.4a and 4.4b for X- and Y-directions, respectively. Storey displacement at top floor is almost the same as calculated target displacement in chapter 3. A comparison of storey displacement at top floor (level 6) for respective earthquake levels is made which gives the following results. In X-direction, an increase of 38.18% and 105.76% has been noticed for DBE and MCE with respect to that of SLE. In Y-direction, an increase of 39.29% and 81.78% is found for DBE and SLE when compared with SLE.

There are minor differences between elastic and inelastic storey displacements at respective EQ levels in both X- and Y-directions. This might be due to different method of evaluation. An other reason for very less difference is because of symmetry in building in both plan and elevation. In case of X-direction, the difference is 8.24%, 1.80%, and 3.53% for SLE, DBE, and MCE, respectively. In Y-direction, the difference is 11.18%, 10.775, and 7.56% for SLE, DBE, and MCE, respectively.

Decrease in storey displacement is observed in Y-direction as compared to that of X-direction for both static linear (EX and EY) and non-linear (Push-X and Push-Y) load cases. In case of ESA, a decrease of 32.29% is observed while in case of PoA a maximum of 38.62% decrease is observed at MCE. The less storey displacements in Y-direction as compared to that of X-direction for all EQ levels is because of dual system and hence more stiffness in Y-direction. Another reason for less displacement in Y-direction as compared to that of X-direction is effective time period. Spectral displacement is directly proportional to effective time period. As effective time period in Y-direction is less than that of X-direction, thus less displacement in Y-direction. Percentage increase in storey displacement for PoA at DBE and MCE as compared to that of SLE is shown in Table 4.4.

TABLE 4.4: Percentage increase in storey displacement at DBE and MCE w.r.t. SLE

	Storey Displacement at	
Load Case	DBE	MCE
Push-X	38.18%	105.76%
Push-Y	39.29%	81.78%

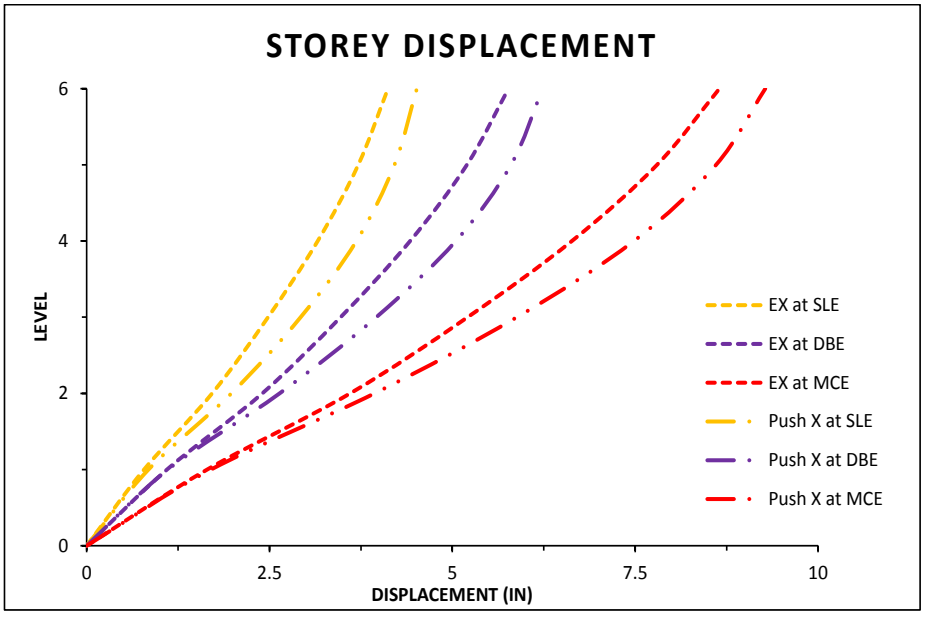

a: Storey Displacement in X-direction

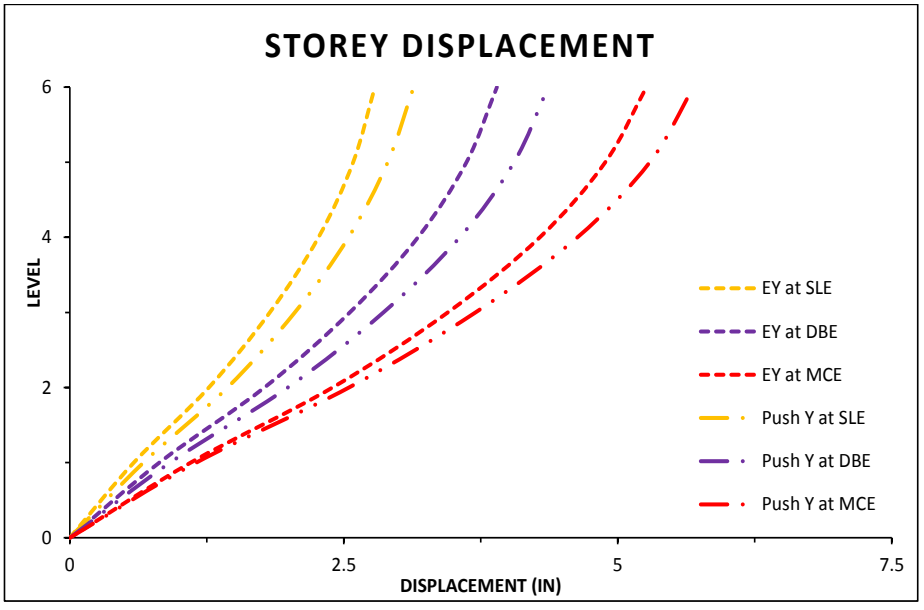

b: Storey Displacement in Y-direction

FIGURE 4.4: (a) Storey displacement in X-direction (b) Storey displacement in Y-direction

4.2.4 Storey Drift

The relative difference of storey displacements between two consecutive floors is known as storey drift. Storey drift at different EQ levels is illustrated in Figures 4.5a and 4.5b for X- and Y-directions, respectively. A comparison of storey drift at governing floor (level 2) for respective earthquake levels is made which gives the following results. In X-direction, there is an increase of 34.66% and 97.18% in storey drift for DBE and MCE as compared to that of SLE. In Y-direction, an increase of 48.05% and 80.52% in storey drift has been observed for DBE and MCE as compared to that of SLE. Storey drift has decreased 33.84% in Y-direction as compared to X-direction in case of ESA. While in case of PoA, storey drift in Y-direction has decreased 37.6% as compared to X-direction. It must be noted that values of storey drift resulting from ESA and PoA are relatively close to each other. The overall storey drift in Y-direction is less than that of X-direction as the storey displacement in Y-direction is less as compared to X-direction, thus less difference in consecutive floor levels. The reasons for less storey drift in Y-direction are less time period in Y-direction and dual system, thus, more stiffness in Y-direction. The storey drift is in accordance to UBC (1997) clause 1630.10.2 in both X- and Y-direction. Percentage increase in storey drift for PoA at DBE and MCE as compared to that of SLE is shown in Table 4.5.

TABLE 4.5: Percentage increase in storey drift at DBE and MCE w.r.t. SLE

	Storey Drift at	
Load Case	DBE	MCE
Push-X	34.66%	97.18%
Push-Y	48.05%	80.5%

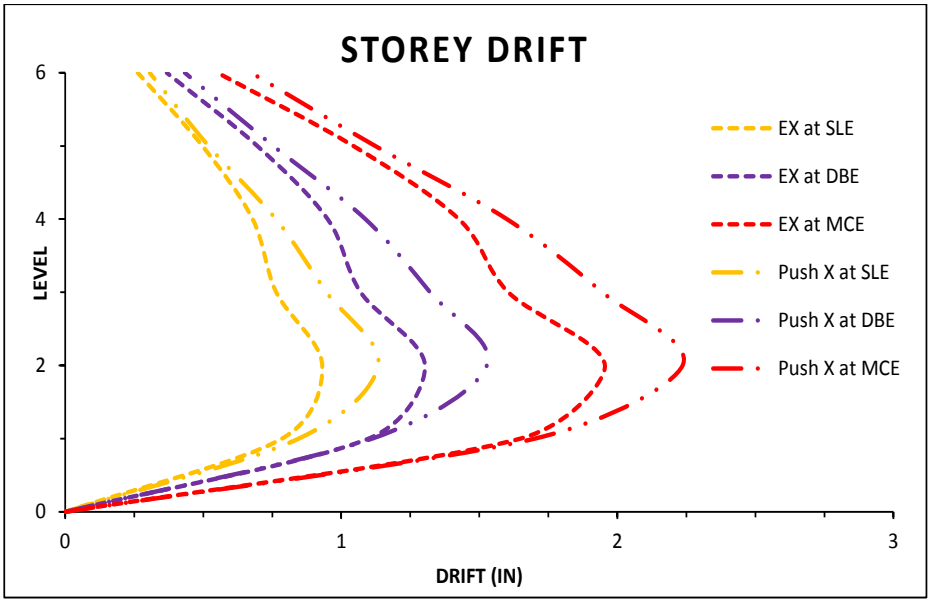

a: Storey Drift in X-direction

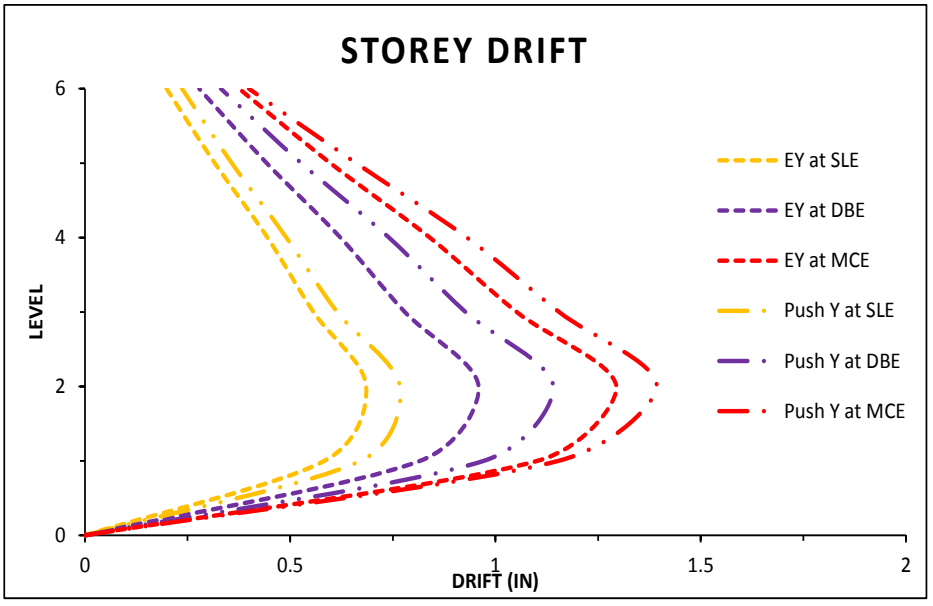

b: Storey Drift in Y-direction

FIGURE 4.5: (a) Storey drift in X-direction (b) Storey drift in Y-direction

4.3 Damage Assessment

As mentioned earlier, seismic damage assessment may be carried out for a number of versatile purposes like seismic design optimization, EQ insurance considerations, and EQ hazard reduction. In the present study, damage assessment is done with

the purpose to quantify the structural damage and estimate the amount of cost and time to restore the building to be functional. Using the methodology described in Chapter 3, damage in beams with respect to beam size, damage state and span length is summarized in Tables 4.6 and 4.7 for different levels of EQ in X- and Y-direction, respectively. Percentages of beams at minor, light and moderate damage states in X- and Y-direction against different EQ intensities is presented in Table 4.8. In X-direction, there are eight types of beams with respect to X-sectional size, three different span lengths and 102 beams in total. Likewise, in Y-direction, there are only two types of beams with respect to X-sectional size, four different span lengths and 104 beams in total. Number of beams in each bay is 34 and 26 for X- and Y-direction, respectively. Number of beams at minor, light and moderate damage state at each EQ level are mentioned at the end of the respective table. It is clear from Tables 4.6 and 4.7 that as the EQ intensity is decreasing from MCE to SLE, number of beams is also increasing from moderate damage state towards light and minor damage states. Even at MCE, there are only 4 (3.92%) and 10 (9.61%) beams at moderate damage state in X- and Y-direction, respectively. Such low percentages of beams at moderate damage state even at MCE signifies the conservativeness of Equivalent Static Analysis (ESA) and Code Based Seismic Design (CBSD) procedures. This might also be because the building is symmetric and self-stable as the the base width to height ratio (slenderness ratio) of the building is very low (1:2).

In X-direction at MCE, there are 2 (1.96%), 96 (94.12%) and 4 (3.92%) beams at minor, light and moderate damage state, respectively. At DBE, there are 12 (11.76%) and 90 (88.24%) beams at minor and light damage state, respectively and no beam is at moderate damage state. At SLE, there are 19 (18.63%) and 83 (81.37) beams at minor and light damage state, respectively and no beam is at moderate damage state.

In Y-direction at MCE, there are 19 (18.26%), 75 (72.12%) and 10 (9.62%) beams at minor, light and moderate damage state, respectively. At DBE, there are 28 (26.92%) and 76 (73.08%) beams at minor and light damage state, respectively and no beam is at moderate damage state. At SLE, there are 47 (45.19%) and 57

(54.81%) beams at minor and light damage state, respectively and no beam is at moderate damage state.

Table 4.6: Damage summary of beams in X-direction

					At MCE				At DBE				At SLE			
Sr. No	Beam Name	Beam Size (in)	Total	Damage State	Span (ft)	Span (ft)	Span (ft)	Sub-total	Span (ft)	Span (ft)	Span (ft)	Sub-total	Span (ft)	Span (ft)	Span (ft)	Sub-total
-	-	-	-	-	8.75	9.25	20.875	-	8.75	9.25	20.875	-	8.75	9.25	20.875	-
1	B1	9x15	7	Minor	0	0	0	0	3	0	0	3	3	0	0	3
				Light	7	0	0	7	4	0	0	4	4	0	0	4
				Moderate	0	0	0	0	0	0	0	0	0	0	0	0
2	B2	9x21	20	Minor	0	0	0	0	0	0	0	0	3	2	2	7
				Light	6	7	7	20	6	7	7	20	3	5	5	13
				Moderate	0	0	0	0	0	0	0	0	0	0	0	0
3	B3	9x54	2	Minor	0	0	0	0	0	0	0	0	0	0	0	0
				Light	2	0	0	2	2	0	0	2	2	0	0	2
				Moderate	0	0	0	0	0	0	0	0	0	0	0	0
4	B4	9x66	4	Minor	0	0	0	0	0	0	0	0	0	0	0	0
				Light	4	0	0	4	4	0	0	4	4	0	0	4

				Moderate	0	0	0	0	0	0	0	0	0	0	0	0
5	B5	9x75	1	Minor	0	0	0	0	0	0	0	0	0	0	0	0
				Light	1	0	0	1	1	0	0	1	1	0	0	1
				Moderate	0	0	0	0	0	0	0	0	0	0	0	0
6	B6	12x12	3	Minor	0	0	0	0	0	1	0	1	0	1	0	1
				Light	1	1	1	3	1	0	1	2	1	0	1	2
				Moderate	0	0	0	0	0	0	0	0	0	0	0	0
7	B7	12x21	65	Minor	0	2	0	2	0	8	0	8	0	8	0	8
				Light	13	24	22	59	13	18	26	57	13	18	26	57
				Moderate	0	0	4	4	0	0	0	0	0	0	0	0
		Grand Total	102	-	34	34	34	102	34	34	34	102	34	34	34	102
				Summary	[Minor = 2]			[Minor = 12]			[Minor = 19]					
					[Light = 96]			[Light = 90]			[Light = 83]					
					[Moderate = 4]			[Moderate = 0]			[Moderate = 0]					

Table 4.7: Damage summary of beams in Y-direction

					At MCE					At DBE					At SLE				
Sr. No	Beam Name	Beam Size (in)	Total	Damage State	Span (ft)	Span (ft)	Span (ft)	Span (ft)	Sub-total	Span (ft)	Span (ft)	Span (ft)	Span (ft)	Sub-total	Span (ft)	Span (ft)	Span (ft)	Span (ft)	Sub-total
-	-	-	-	-	10.375	12.25	9.875	6.75	-	10.375	12.25	9.875	6.75	-	10.375	12.25	9.875	6.75	-
1	B2	9x21	52	Minor	7	2	6	0	15	7	2	6	0	15	7	6	6	6	25
				Light	6	11	7	13	37	6	11	7	13	37	6	7	7	7	27
				Moderate	0	0	0	0	0	0	0	0	0	0	0	0	0	0	0
2	B7	12x21	52	Minor	0	0	0	4	4	0	0	0	13	13	0	9	0	13	22
				Light	9	13	7	9	38	13	13	13	0	39	13	4	13	0	30
				Moderate	4	0	6	0	10	0	0	0	0	0	0	0	0	0	0
	[Grand Total]		104	-	26	26	26	26	104	26	26	26	26	104	26	26	26	26	104
				Summary	[Minor =	19]	[Minor =	28]		[Minor =	47]								
					[Light =	75]	[Light =	76]		[Light =	57]								
					[Moderate =	10]	[Moderate	0]		[Moderate	0]								

TABLE 4.8: Percentages of beams at different damage states

		EQ Level		
Orientation	Damage State	MCE	DBE	SLE
X-direction	Minor	1.96%	11.76%	18.63%
	Light	94.12%	88.24%	81.37%
	Moderate	3.92%	0%	0%
Y-direction	Minor	18.26%	26.9%	45.19%
	Light	72.12%	73.08%	54.81%
	Moderate	9.62%	0%	0%

Classification of columns with respect to column size and damage state for different levels of EQ in X- and Y-directions is represented in Table 4.9. Damage of only ground floor columns is assessed as hinges were assigned only to these columns. There are total 16 columns with five different X-sectional sizes. The summary of overall damage in beams and columns is shown in graphical manner in Figures 4.6 and 4.7, respectively.

In X-direction, there is no column at moderate damage state. At MCE, all 16 columns are at light damage state while at SLE, all 16 columns are at minor damage state. At DBE, there are 9 and 7 columns at minor and light damage state, respectively.

In Y-direction at MCE, there are 2, 9 and 5 columns at minor, light and moderate damage state, respectively. At DBE, , there are 9 and 7 columns at minor and light damage state, respectively. While at SLE, all 16 columns are at minor damage state. It is clear from Table 4.8 that damage state pattern at DBE and SLE is identical in both X- and Y-direction. The results confirm that the building had been designed on the strong-column-weak-beam principle.

TABLE 4.9: Damage summary of columns in X- and Y-direction

					X-direction			Y-direction		
Sr. No	Column Name	Column Size (in)	Total	Damage State	At MCE	At DBE	At SLE	At MCE	At DBE	At SLE
1	C1A (12-6)	15x2	4	Minor	0	2	4	0	2	4
				Light	4	2	0	2	2	0
				Moderate	0	0	0	2	0	0
2	C1B (10-6)	15x21	7	Minor	0	4	7	0	3	7
				Light	7	3	0	5	4	0
				Moderate	0	0	0	2	0	0
3	C2	18x24	1	Minor	0	1	1	0	1	1
				Light	1	0	0	1	0	0
				Moderate	0	0	0	0	0	0
4	C4	21x21	2	Minor	0	1	2	0	1	2
				Light	2	1	0	1	1	0
				Moderate	0	0	0	1	0	0
5	C7	33x9	2	Minor	0	1	2	2	2	2
				Light	2	1	0	0	0	0
				Moderate	0	0	0	0	0	0
	[Grand	Total]	16	-	16	16	16	16	16	16
		Summary		Minor	0	9	16	2	9	16
				Light	16	7	0	9	7	0
				Moderate	0	0	0	5	0	0

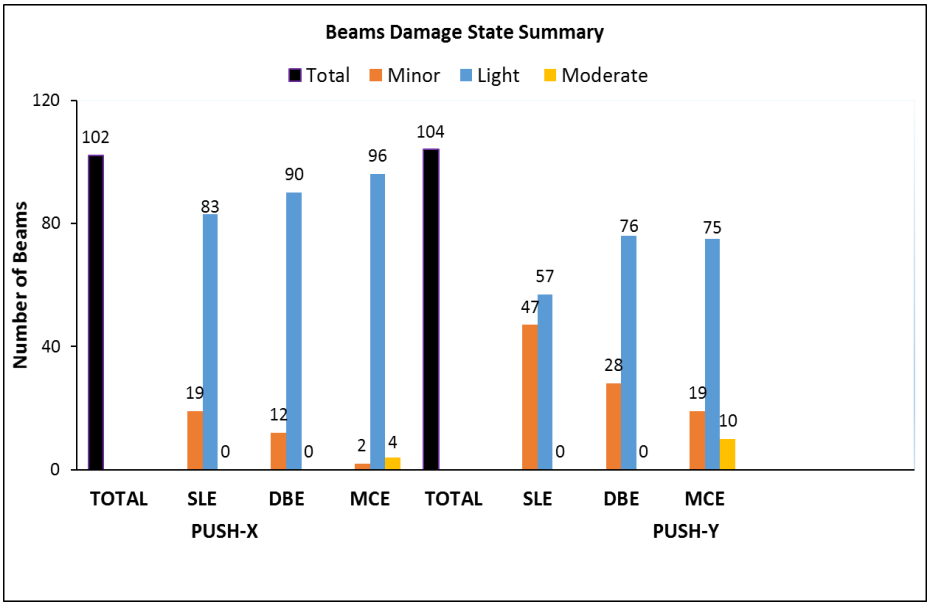

FIGURE 4.6: Beams damage state summary

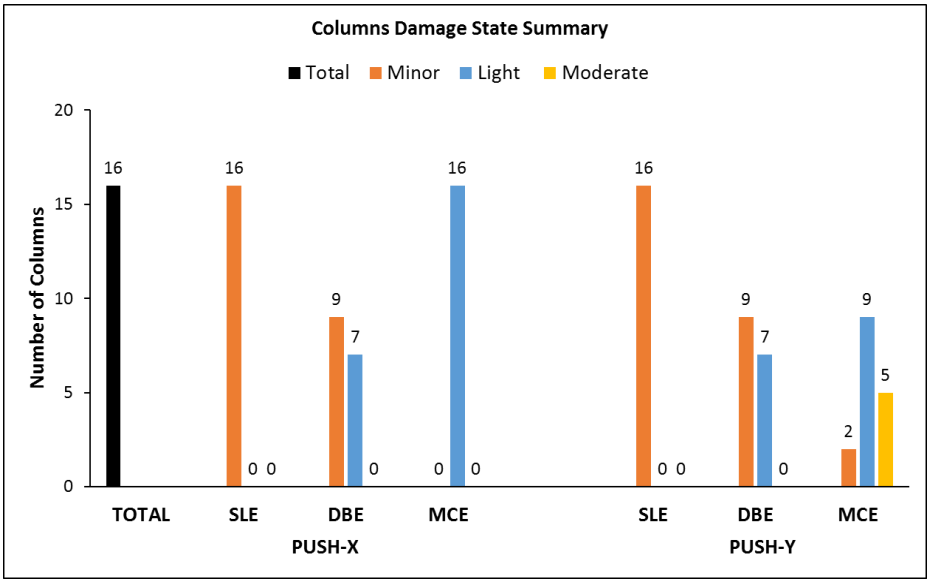

FIGURE 4.7: Columns damage state summary

4.4 Cost and Time Calculation

A building needs to be restored to pre-earthquake condition in terms of strength and stiffness to be functional and safe for inhibitants. It can be done by applying

retrofit or repair techniques. In the former, system is upgrated by adding a new element to increase the strength and stiffnesss. This includes adding shear walls, braced frames, buttresses and jacketing etc. The later includes the strengthing of damaged structural members without adding a new element to the system. It includes epoxy injection, chiken wire mesh, CFRP sheets and CFRP strips etc. Guidelines for these techniques are outlined in detail in FEMA-356 (2000) and ATC-40 (1996) documents. In the present research project, based on literature, FEMA-356 (2000) and ATC-440 (1996) guidelines and local maket survey (Sika, Spit, Hilti, Imporient Chemicals), use of chiken wire mesh, epoxy injection and CFRP sheets is recommended for minor, light and moderate damage state, respectively. Composite rates (cost of material+labour+scaffolding) of these materials are taken from local market survay. As there is no research in available literature that propose a relationship between any seismic engineering parameter (stress, strain, hinge rotation, base shear, roof displacement, storey drift etc) and number of cracks occurred in structural component of a building, number of cracks occurred are supposed to be 2, 4, and 6 for negligible, light, and moderate damage state, respectively. Repair remedy adopted for different damage states along with assumed number of cracks is shown in Table 4.10.

TABLE 4.10: Repair technique and unit rate for different damage states

Damage State	Repair Technique	No. of cracks Assumed	Unit Rat (PKR)
Minor	Chisling, chipping off plaster and chiken wire mesh	2	150/ft
Light	Low viscosity epoxy injection	4	1000/ft
Moderate	Low viscosity epoxy injection + CFRP wrap	6	1000/ft + 1000/sft

Epoxy injection is widely used and recommended procedure for restoring structural strength. Low viscosity epoxy injection is used to fill and seal cracks. It not only forms an effective barrier against water infiltration of corrosion promoting elements, but also bonds the concrete sections together. Epoxy injection is highly technical work and requires skill and care in executing it. First weak area around crack is chipped off. Crack surface is cleaned with wire brush to make it free of

any dust or dirt. Inlet and outlet injection nozzles are fixed on the prepared crack surface and the remaining crack surface is sealed with epoxy adhesive to make the crack leakage free. Epoxy injection is initiated after at least 24 hours of nozzles fixing. Then epoxy is injected via injection pump until it seeps out of the outlet nozzle. Nozzles are corked and the injected cracks are left to cure for 24 hours. Crack length is determined from the x-sectional dimensions of the component. Cost of epoxy injection is then obtained from the product of crack length, number of cracks, and unit price.

Carbon fiber reinforced polymer (CFRP) wrap is an extremely strong and light-weight plastic which contains cabon fibers. It is used to increase the flexural and shear load capacity of structural components as well as ductilty of columns. It is available in ready-to-use form and its application is very easy and simple. The surface, on which CFRP wrap is to be applied, is grinded and made dust free as it needs a good and uniform concrete bonding surface. The surface of application is primed with epoxy with the help of roller. The CFRP wrap is cut as per desired length and epoxy is applied on the wrap as well. The CFRP wrap is then applied on the the surface and pressed hard to remove any voids and gaps with the help of a special roller. Cost is calculated by multiplying area of CFRP wrap with unit price of CFRP.

Cost analysis is carried out to approximate the amount required for rehabilitation of building in comparison to the construction amount of building. Cost comparison in the present study is only for grey structure. Actual cost is approximated by taking the quantities of concrete and steel used in the building. Volume of concrete is taken from SAP-2000 by dividing the total weight of structural components by the density of RC concrete. Quantity of steel is calculated emperically using the the quantity of concrete. Actual cost is calculated by taking product of quantities with unit rates of concrete and steel. Labour cost, as per current market rates, is also incorporated in actual construction cost. Repair cost is calculated as per damage state of structural member, repair technique used and unit rate as described in Table 4.10. A relative structural cost comparison at different intensities of earthquake is represented in Figure 4.8. Repair cost comes out to be 26%,

17%, and 14% of the total construction cost for maximum considered, designed based, and service level earthquake, respectively. Even at MCE, only 26% repair cost indicates the conservativeness of the code based design and the building has reserved capacity to a great extent. It must be noted that relative structure cost percntages are as per current market rates that might be subjected to change for different repair techniques at clients discretion or from time to time.

Time required for repair works is estimated, as per current market survey, by considering a team of 3 technical persons working for 8 hours per working day. The estimated duration may vary depending on the number of persons working. Number of beams at minor damage state completed in one working day is 6 while for columns, it is taken as 4. For light and moderate damage state, beams and columns completed in one working day is 3. Values are rounded off to nearest whole number to make calculations simple and easy. Details of durations for different earthquake levels considering number of beams and columns at different damage states is illustrated in Table 4.11 and graphically represented in Figure 4.9.

Table 4.11: No. of days required for repair works

Sr. No	EQ Level	Damage State	No. of Beams	No. of Days	Total No. of Days	No. of Columns	No. of Days	Total No. of Days
1	MCE	Minor	21	4	66	2	1	6
		Light	171	57	-	9	3	-
		Moderate	14	5	-	5	2	-
2	DBE	Minor	40	7	62	9	3	5
		Light	166	55	-	7	2	-
		Moderate	0	0	-	0	0	-
3	SLE	Minor	66	11	58	16	4	4
		Light	140	47	-	0	0	-
		Moderate	0	0	-	0	0	-

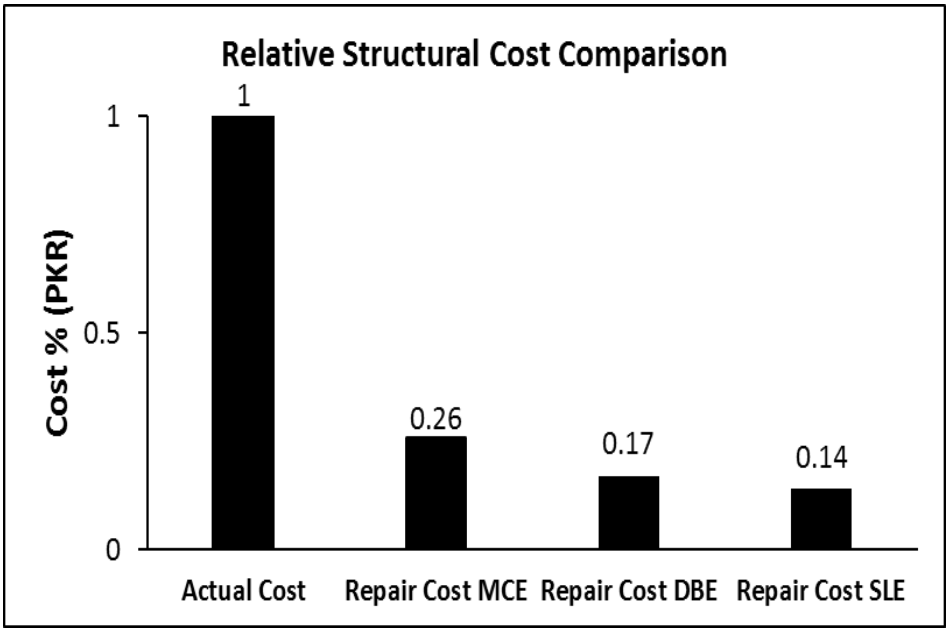

FIGURE 4.8: Relative structure cost comparison at MCE, DBE and SLE

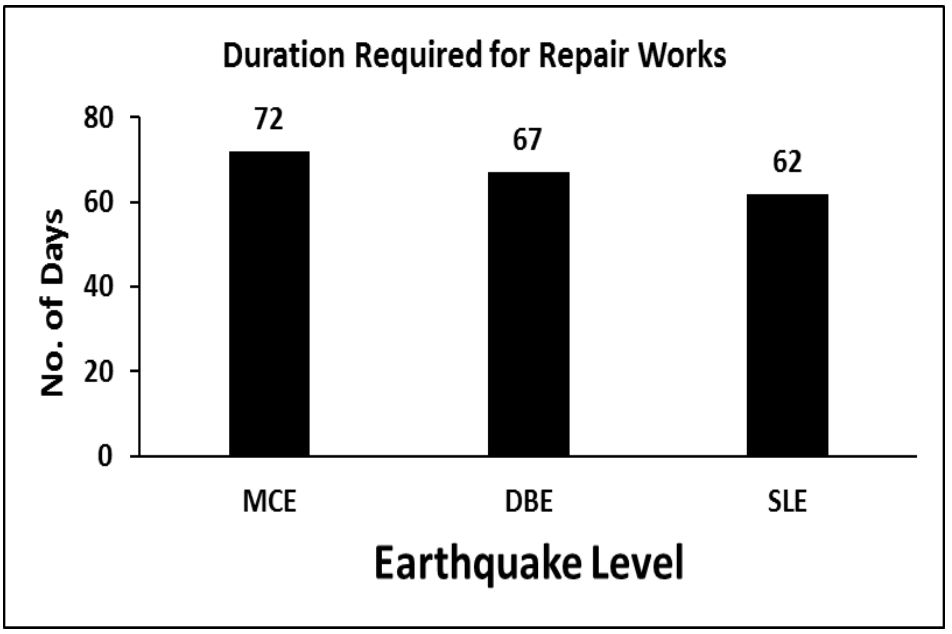

FIGURE 4.9: Estimated durations for repair works at MCE, DBE and SLE

4.5 Summary

In the current chapter, results of the research project are presented and discussed in details. Results of seismic response parameters i.e. storey shear, storey overturning moment, storey displacement, and storey drift are discussed and graphically presented. Number of beams and columns at different damage states are calculated and summarized. Remedy suggestions for different damage states are recommended based on literature and market survey. Methodology for recommended suggestions is described. Time and cost analysis is done for the damage. From results, it is clear that non-linear static PoA is a better and rational method for analysis and help to better understand the seismic behavior of structure. Results show that even at MCE, the damage percentage is only 26% which indicates the conservativeness of the conventional codes used for analysis and design. Code based design is conservative and underestimates the capacity and seismic behavior of the structure in terms of seismic response parameters. There is need to switch from linear static to nonlinear static/dynamic analysis procedures to get more rational, realistic and economic solutions in order to achieve the desired performance objective.

Chapter 5

Conclusions and Recommendations

In the current case study, an attempt has been made to assess the seismic damage in a quantifiable manner and to estimate the repair cost for service level, designed based, and maximum considered earthquakes. In addition to damage and cost assessment, seismic performance of the building is also evaluated and compared in terms of seismic response parameters such as storey shear, moment, displacement, and drift. For this an existing mid-rise 7 storey reinforced concrete frame building, located in seismic zone 2B with soil profile type S_D, is analyzed and designed by equivalent static analysis procedure of UBC (1997) and ACI-318 (2008), respectively. A non-linear model of the same building is prepared by assigning plastic hinges at suitable locations. The model is analyzed by PoA method in X- and Y-directions as per FEMA-356 (2000) provisions. Strain is determined for calculation of crack width classifying the structural components into different damage states. Based on the numerical assessment, following conclusions can be drawn from the study.

5.1 Conclusions

- Time period of the building by Method A from ESA is same for all models in both X- and Y-direction. The reason for same time period is the limitation of code based time period using Method A that incorporates only height of the building. However, time period from Method B, calculated by the software, comes out to be 1.03 sec and 0.59 sec for X- and Y-direction, respectively. The reason for less time period in Y-direction is more stiffness due to shear walls in Y-direction.

- In X-direction, target displacement calculated for SLE, DBE, and MCE is 4.25 in, 5.89 in, and 8.94 in, respectively. While in Y-direction, target displacement comes out to be 2.18 in, 3.49 in, and 5.23 in for SLE, DBE, and MCE, respectively. The reason for less target displacements in Y-direction as compared to that of X-direction is less time period in Y-direction as compared to X-direction.

- There is significant difference between locations of center of mass and center of rigidity due to presence of shear wall and massive and closely spaced columns towards the right half of the case study building. A number of advantages might have achieved in analysis and design if there had been less difference between center of mass and center of rigidity like more stability and safety, less drift, less torsional moments, optimal cross sectional sizes, economization of structural cost, enhanced seismic performance etc.

- Storey shear from ESA for all models is approximately the same in both X- and Y-direction. However, storey shear has increased upto 14.84% in Y-direction as compared to that of X-direction in case of PoA. This is because the building has less time period and more stiffness in Y-direction due to shear walls. In case of PoA in X-direction, storey shear has increased 12.49% and 27.33% for DBE and MCE with respect to SLE. While in Y-direction, storey shear has increased by 13.09% and 39.90% when compared to that of SLE. Reason for increased storey shear at DBE and MCE is as the intensity of EQ increases, base shear increases and thus, the storey shear.

- Over-turning moment from ESA is approximately the same for all models in both X- and Y-direction. In case of PoA in X-direction, storey over-turning moment has increased 24.22% and 66.46% for DBE and MCE with respect to SLE. While in Y-direction, storey over-turning moment has increased by 31.31% and 86.83% when compared to that of SLE. The reason for increase is that over-turning moment is the function of lateral force distribution. As the lateral force increases for DBE and MCE, over-turning moment increases.

- Elastic storey displacement in case of EX is same for all models and the same pattern is observed in case of EY. However, inelastic storey displacement for load case Push-X has been increased by 38.18% and 105.76% for DBE and MCE in comparison to SLE. While for load case Push-Y, inelastic displacement is increased by 39.29% and 81.78% for DBE and MCE with respect to SLE.

- Decrease in storey displacement is observed in Y-direction as compared to that of X-direction for both static linear (EX and EY) and non-linear (Push-X and Push-Y) load cases. In case of ESA, a decrease of 32.29% is observed while in case of PoA, a maximum of 38.62% decrease is observed at MCE. The reason for decrease in storey displacement is more stiffness due to shear walls in Y-direction. An other reason for less displacement in Y-direction as compared to that of X-direction is effective time period. Spectral displacement is directly proportional to effective time period. As effective time period in Y-direction is less than that of X-direction, thus less displacement in Y-direction.

- Storey drift is increased 34.66% and 97.18% for DBE and MCE as compared to that of SLE for load case Push-X. For load case Push-Y, an increase of 48.05% and 80.50% is observed for DBE and SLE in comparison to SLE.

- At MCE in X-direction, there are 2 (1.96%), 96 (94.12%), and 4 (3.92%) beams at negligible, light, and moderate damage state, respectively. While in Y-direction, there are 19 (18.27%), 75 (72.12%), and 10 (9.61%) beams at negligible, light, and moderate damage state, respectively.

- At DBE in X-direction, there are 12 (11.76%), and 90 (88.24%) beams at negligible, and light damage state, respectively. While in Y-direction, there are 28 (26.92%), and 76 (73.08%) beams at negligible, and light damage state, respectively. There are no beams at moderate damage state in X- and Y-directions.

- At SLE in X-direction, there are 19 (18.63%), and 83 (81.37%) beams at negligible, and light damage state, respectively. While in Y-direction, there are 47 (45.19%), and 57 (54.81%) beams at negligible, and light damage state, respectively. There are no beams at moderate damage state in X- and Y-directions.

- At MCE in X-direction, all 16 (100%) columns are at light damage state. While in Y-direction, there are 2 (12.50%), 9 (56.25%), and 5 (31.25%) columns at negligible, light, and moderate damage state, respectively.

- At DBE, there are 9 (56.25%) and 7 (43.75%) columns at negligible, and light damage state, respectively, in both X- and Y-directions.

- At SLE, all 16 (100%) columns ate at negligible damage state, in both X- and Y-directions.

- The estimated repair cost at MCE, DBE, and SLE comes out to be 26%, 17%, and 14%, respectively, relative to the actual structural cost. The 26% repair cost even at MCE indicates that the building has a reserved capacity to a great extent.

- The time duration for repair works is estimated 74, 67, and 62 days for MCE, DBE, and SLE, respectively.

- The plastic hinge rotation of beams and columns comply well with the acceptance criteria of FEMA-356 (2000) Table 6-7 and 6-8, respectively.

- Code based design is conservative and underestimates the capacity and seismic behavior of the structure in terms of seismic response parameters. There

is need to switch from linear static to nonlinear static/dynamic analysis procedures to get more rational, realistic and economic solutions in order to achieve the desired performance objective.

5.2 Future Recommendations

The core objective of the current research project was to evaluate the structural damage at different hazard levels and estimate the cost and time for rehabilitation. To do so, non-linearity has been induced at specified locations only and only non-linear static push-over analysis is performed. Further research can be carried out by assigning fiber hinges throughout the frame and area elements. Effect of load bearing infill walls, non-load bearing partition walls and other non-structural elements may be considered for more precise damage assessment. Non-linear dynamic time history analysis can be performed for more rational analysis of the building in terms of damage assessment. In the present study, number of cracks has been assumed for estimation of repair cost. A research can be done about correlation between seismic response parameters and number of cracks.

Bibliography

ACI Committee 318, (2008). Building Code Requirements for Structural Concrete and Commentary, (ACI 318M-08). American Concrete Institute, Farmington Hills, MI

ACI Committee E706, (2009). Structural Crack Repair by Epoxy Injection (ACI RAP-1). American Concrete Institute, Farmington Hills, MI

Andres, L. L., T. Antonio, and S. O. Gregorio, (2016). Influence of adjusted models of plastic hinges in nonlinear behaviour of reinforced concrete buildings. Engineering Structures, Vol: 124, pp: 245-57

Antoniou, S., (2002). Advanced Inelastic Static Analysis for Seismic Assessment of Structures. PhD Thesis, Engineering Seismology and Earthquake Engineering Section, Imperial College, London, United Kingdom.

ASCE STANDARDS. ASCE/SEI 41-07, (2007). Seismic Rehabilitation of Existing Buildings. American Society of Civil Engineers. pp: 1-550

ATC-32, (1996). Improved seismic design criteria for California bridges. Applied Technology Council. Provisional recommendations. Redwood City (CA). pp: 1-215

ATC-40, (1996). Seismic Evaluation and Retrofit of Concrete Buildings. Report (ATC-40), Applied Technology Council, California, USA. Vol: 1

Bae S. and Bayrak O., (2008). Plastic Hinge Length of Reinforced Concrete Columns. ACI Structural Journal, Vol: 105, Issue: 3, pp: 290-300

Baker ALL, (1956). Ultimate load theory applied to the design of reinforced and prestressed concrete frames. Concrete Publications Ltd., London. pp: 1-91

Bayuaji R., Darmawan M. S., Husin N. A., Anugraha R. B., Budipriyanto A., and Stewart M. G., (2018). Corrosion damage assessment of a reinforced concrete canal structure of power plant after 20 years of exposure in a marine environment: A case study. Engineering Failure Analysis, Vol: 84, pp: 287-299

Bracci, J.M., Reinhorn, A.M., Mander, J.B. and Kunnath, S.K., (1989). Deterministic model for seismic damage evaluation of RC structures, Technical Report NCEER-89-0033, State University of New York, Buffalo NY, USA. Earthquake Engineering to Extreme Events, pp: 1-106

BCP, (2007). Building Code of Pakistan, Seismic provisions, 2007. Ministry of Housing and Public Works, Government of Islamic Republic of Pakistan. pp: 1-268

Coleman J and Spacone E, (2001). Localization issues in force-based frame elements. Journal of Structural Engineering, Vol: 127, Issue: 11, pp: 1257-1265

Computers and Structures, (2006). Perform 3D, Nonlinear Analysis and Performance Assessment for 3D Structures User Guide, Version 4. Computers and Structures, Inc.: Berkeley, CA, 2006.

Corley GW, (1966). Rotation capacity of reinforced concrete beams. ASCE Journal of Structural Division, Vol: 92, Issue: 5, pp: 121-146

CTBUH, (2008). Recommendations for the Seismic Design of High-rise Buildings. A Consensus Document, Council on Tall Buildings and Urban Habitat, Seismic Working Group, 2008. pp: 1-28

Daniyal, M., Akhtar, S., (2020). Corrosion assessment and control techniques for reinforced concrete structures: a review. Journal of Building Pathology and Rehabilitation, Vol: 5, Issue: 1, pp: 1-20

Di Julio, R. M., (2001). Linear static seismic lateral force procedures. In The Seismic Design Handbook, pp: 247-273

Elenas A., and Meskouris K., (2001). Correlation study between seismic acceleration parameters and damage indices of structures. Engineering Structures, Vol: 23, Issue: 6, pp: 698-704

Elnashai, A.S., (2001). Advanced inelastic static (pushover) analysis for earthquake applications. Structural Engineering and Mechanics, Vol: 12, Issue: 1, pp: 51-69

Erduran E., Lang D.H., Lindholm D. C., Toma-Denila D., Balan S. F., Ionescu V., Aldea A., Vacareanu R., and Neagu C., (2012). Real-Time Earthquake Damage Assessment in the Romanian-Bulgarian Border Region. Proceedings of the 15th World Conference on Earthquake Engineering (WCEE), Lisbon. Paper No. 3945, pp: 1-10

Erduran, E. and Yakut, A., (2004). Drift based damage functions for reinforced concrete columns. Computers and Structures, Vol: 82, Issue: 2, pp: 121-130

Fajfar, P., (2002). Structural analysis in earthquake engineering. A breakthrough of simplified non-linear method. 12th European Conference on Earthquake Engineering, Paper Ref: 843 (2002), pp: 1-20

Fardis MN, Biskinis DE, (2003). Deformation of RC members, as controlled by flexure or shear. In: Proceedings of the international symposium honouring Shunsuke Otani on performance-based engineering for earthquake resistant reinforced concrete structures.

Farouk, M.A. and Khalil, K.F., (2020). Alternative mathematical modeling for plastic hinge of reinforced concrete beam. SN Applied Sciences, Vol: 2, Issue 6, pp: 1-13

FEMA-273, (1997). NEHRP guidelines for the seismic rehabilitation of buildings. Federal Emergency Management Agency, Washington DC, USA

FEMA-308, (1999). Repair of earthquake damaged concrete and masonry wall buildings. Federal Emergency Management Agency, Washington DC, USA

FEMA-356, (2000). Pre-standard and Commentary for the Seismic Rehabilitation of Buildings. Federal Emergency Management Agency, Washington DC, USA

FEMA-369, (2001). NEHRP Recommended Provisions for Seismic Regulations for New Buildings and Other Structures. Federal Emergency Management Agency, Washington DC, USA

FEMA-440, (2005). Improvement of Nonlinear Static Seismic Analysis Procedure. Federal Emergency Management Agency, Washington DC, USA

FEMA-445, (2006). Next-generation Performance Based Seismic Design Guidelines. Federal Emergency Management Agency, Washington DC, USA

FEMA-450, (2003). NEHRP Recommended Provisions and Commentary for Seismic Regulations for New Buildings and Other Structures. Federal Emergency Management Agency, Washington DC, USA

Freeman, S.A., Nicoletti, J.P., and Tyrell, J.V., (1975). Evaluations of existing buildings for seismic risk: A case study of Puget Sound Naval Shipyard, Bremerton, Washington. In Proceedings of U.S. National Conference on Earthquake Engineering, Earthquake Engineering Research Institute (EERI), Berkeley. Earthquake Engineering, pp: 113-122

Freeman, S.A., (1978). Prediction of Response of Concrete Buildings to Severe Earthquake Motion. ACI Structural Journal, Vol: 55, Issue: 2, pp: 589-605

Frosch, R.J., (1999). Another look at cracking and crack control in reinforced concrete. ACI Structural Journal, Vol: 96, Issue: 3, pp: 437-442

Gergely, P. and Lutz, L.A., (1968). Maximum crack width in reinforced concrete flexural members. Causes, Mechanism, and Control of Cracking in Concrete. ACI Structural Journal, Vol: 20, Issue: 2, pp: 87-117

Ghobarah, A., Abou-Elfath, H. and Buddha, A., (1999). Response-based damage assessment of structures. Earthquake Engineering and Structural Dynamics, Vol: 28, Issue: 1, pp: 79-104.

Giannopoulos, P.I., (2009). Seismic assessment of RC building according to FEMA 356 and Eurocode 8. In: 16th Conference on Concrete, TEE, ETEK, 21-23/10/2009

Goel, S. C., Liao, W. C., Reza Bayat, M., and Chao, S. H., (2010). Performance based plastic design (PBPD) method for earthquake resistant structures: an overview. The structural design of tall and special buildings, Vol: 19, Issue: 1-2, pp: 115-137

Georgoussis, G. K., (2020). Suggestions for Optimal Seismic Design of Wall-Frame Concrete Structures. Geotechnical, Geological and Earthquake Engineering, Vol: 48, Issue: 3, pp: 321-334

Guo, H., Dong, Y., and Gu, X., (2020). Durability assessment of reinforced concrete structures considering global warming: A performance-based engineering and experimental approach. Construction and Building Materials, Vol: 233, Issue: 1, pp: 117-135

Hait P., Sil A., and Choudhury S., (2020). Damage Assessment of Reinforced Concrete Framed Building Considering Multiple Demand Parameters in Indian Codal Provisions. Iranian Journal of Science and Technology, Transactions of Civil Engineering, Vol: 12, Issue: 2, pp: 54-73

Hakim, R.A., Alama, M. S. and Ashour, S. A., (2014). Seismic Assessment of RC Building According to ATC 40, FEMA 356 and FEMA 440. Arabian Journal for Science and Engineering, Vol: 39, Issue: 3, pp: 7691-7699

HAZUS, (1999). Earthquake loss estimation Methodology HAZUS99 Service Release 2 (SR2) Technical Manual, Federal Emergency Management Agency, Washington DC, USA

Inel, Mehmet and Ozmen, Hayri, (2006). Effects of plastic hinge properties in nonlinear analysis of reinforced concrete buildings. Engineering Structures, Vol: 28, Issue: 11, pp: 1494-1502

ICC PC, (2012). International Building Code (IBC), 12th Edition. International Code Council, Country Club Hills.

Jalilkhani, M., Ghasemi, S. H., and Danesh, M., (2020). A multi-mode adaptive pushover analysis procedure for estimating the seismic demands of RC moment-resisting frames. Engineering Structures, Vol: 213, Issue: 13, pp: 643-661

Kadid A. and Boumrkik A., (2008). Pushover analysis of reinforced concrete frame structures. Asian Journal of civil engineering (building and housing), Vol: 9, Issue: 1, pp: 47-59

Kappos A. J., (1997). Seismic damage indices for RC buildings: evaluation of concepts and procedures. Structural Engineering and Materials, Vol: 1, Issue: 1, pp: 78-87

King, S.A., Hortacsu A., and Hart, G.C., (2004). Post-earthquake estimation of site-specific strong ground motion. 13th World Conference on Earthquake Engineering (WCEE), Canada. Paper No. 2834, pp: 1-13

Komeili, Mehdi and Milani, Abbas and Tesfamariam, Solomon, (2012). Performance based earthquake engineering design of reinforced concrete structures using black-box optimisation. Materials and Structural Integrity, Vol: 6, Issue: 1, pp: 1-25

Kostinakis, Konstantinos and Athanatopoulou, A. and Avramidis, Ioannis, (2013). Evaluation of inelastic response of 3D single-story R/C frames under bidirectional excitation using different orientation schemes. Earthquake Engineering, Vol: 11, Issue: 4, pp: 637-661

Kramer, S.L., (1996). Geotechnical Earthquake Engineering. Prentice Hall civil engineering and engineering mechanics series, ISBN 0-13-374943-6.

Lombard J., Lau D.T., Humar J.L., Foo S., and Cheung M.S., (2000). Seismic Strengthening and Repair of Reinforced Concrete Shear Walls. 12th World Conference on Earthquake Engineering (WCEE), Lisbon. Paper No. 2032, pp: 1-8

Maeda M., Nakano Y., Lee K S., (2004). Post-Earthquake Damage Evaluation for R/C Buildings Based on Residual Seismic Capacity. The 13th World Conference on Earthquake Engineering (WCEE), Canada. August 1-6, 2004. Paper No. 1179, pp: 1-15

Marder, K. J., Elwood, K. J., Motter, C. J., and Clifton, G. C., (2020). Quantifying the effects of epoxy repair of reinforced concrete plastic hinges. Earthquake Engineering, Vol: 53, Issue: 1, pp: 37-51

Martino, R.; Spacone, E.; Kingsley, G., (2000). Nonlinear pushover analysis of RC structures. Advanced Technology in Structural Engineering, Vol: 18, Issue: 4, pp: 223-230

Mattock AH, (1964). Rotational Capacity of Hinging Regions in Reinforced Concrete Beams. Flexural Mechanics of Reinforced Concrete. SP-12, ACI Structural Journal, Vol: 12, Issue: 3, pp: 143-181

Moehle J. P., (2008). Performance-Based Seismic Design of Tall Buildings in the U.S. 14th World Conference on Earthquake Engineering (WCEE), China. October 12-17, 2008. Paper No. 1351, pp: 1-8

Molina, S., Lang, D.H., Lingvall, F., and Lindholm, C.D., (2009). User Manual for the Earthquake Loss Estimation Tool SELENA, v5.0.

Molina, S., Lang, D.H., and Lindholm, C.D., (2010). SELENA An open-source tool for seismic risk and loss assessment using a logic tree computation procedure. Computer and Geosciences, Vol: 36, Issue: 3, pp: 257-269

Ning, F., Mickleborough, N. C., and Chan, C. M., (1999). The effective stiffness of reinforced concrete flexural members under service load conditions. Australian Journal of Structural Engineering, Vol: 2, Issue: 2, pp: 135-144

Niu, Di-tao. and Ren, Li-jie, (1996). A modified seismic damage model with double variables for reinforced concrete structures. Journal of Earthquake Engineering and Engineering Vibration, Vol: 16, Issue: 3, pp: 44-55

Panagiotakos TB and Fardis MN, (2001). Deformations of reinforced concrete members at yielding and ultimate. ACI Structural Journal, Vol: 98, Issue: 2, pp: 135-148

Park, Y. and Ang, A., (1985). Mechanistic seismic damage model for reinforced concrete. ASCE Journal of Structural Engineering, Vol: 111, Issue: 4, pp: 722-739

Park R and Paulay T, (1975). Reinforced Concrete Structures. John Wiley and Sons, New York. 769 pages

Paulay T and Priestley MJN (1992). Seismic Design of Reinforced Concrete and Masonry Buildings. John Wiley and Sons, New York. 767 pages

Poluraju P. and Rao N., (2011). Pushover analysis of reinforced concrete frame structure using SAP-2000. International Journal of Earth Sciences and Engineering, Vol: 4, Issue 2, pp: 684-690

Priestley MJN and Park R, (1987). Strength and ductility of concrete bridge columns under seismic loading. ACI Structural Journal, Vol: 84, Issue: 1, pp: 61-76

Priestley MJN, Seible F, Calvi GMS, (1996). Seismic design and retrofit of bridges. New Zealand Society for Earthquake Engineering, Vol: 33, Issue: 3, pp: 265-285

Reinhorn AM, Kunnath KS, and Valles-Mattox R., (1996). IDARC 2D version 4.0; user manual. State University of New York at Buffalo; Department of Civil Engineering, 1996.

Ren, L., Fang, B., Wang, K., and Yuan, F., (2020). Numerical Investigation on Plastic Hinge Length of Ultra-high Performance Concrete Column under Cyclic Load. Journal of Earthquake Engineering, Vol: 10, Issue: 4, pp: 1-19

Roufaiel, M.S.L. and Meyer, C., (1987). Reliability of concrete frames damaged by earthquakes. ASCE Journal of Structural Engineering, Vol: 113, Issue: 3, pp: 445-457

Sawyer HA, (1964). Design of concrete frames for two failure states. ACI Structural Journal, Vol: 12, Issue: 5, pp: 405-437

Sengupta, Piyali, (2014). Hysteresis Models and Fragility Assessments of Reinforced Concrete Structural Components. Doctoral Thesis, Nanyang Technological University, Singapore. https://hdl.handle.net/10356/60616

Sheikh SA and Khoury SS, (1993). Confined Concrete Columns with Stubs. ACI Structural Journal, Vol: 90, Issue: 4, pp: 414-431

Simsir C.C., Ekwueme C., Hart G.C., and Dumortier A., (2012). Earthquake Damage Assessment of Reinforced concrete Hotel Buildings in Hawaii. 15th World Conference on Earthquake Engineering (WCEE), Lisbon. Paper No. 3890, pp: 1-10

Sinha, R. and Goyal, A., (2004). A national policy of seismic vulnerability assessment of buildings and procedure for rapid visual screening of buildings for potential seismic vulnerability. Department of Civil Engineering, IIT Bombay. pp: 1-12

Sinha R., and Shiradhonkar S. R., (2012). Seismic Damage Index for Classification of Structural Damage Closing the Loop. 15th World Conference on Earthquake Engineering (WCEE), Lisbon. Paper No. 3479, pp: 1-10

Tabeshpour, Mohammad amd Bakhshi, Ali and Golafshani, A., (2004). Vulnerability and damage analyses of existing buildings. 13th World Conference on Earthquake Engineering (WCEE), Canada. Paper No. 1261, pp: 1-13

Tehranizadeh M, and Moshref A., (2011). Performance-based optimization of steel moment resisting frames. Scientia Iranica, Vol: 18, Issue: 2, pp: 198-204

Thai, D., Pham, T., and Nguyen, D., (2020). Damage assessment of reinforced concrete columns retrofitted by steel jacket under blast loading. The Structural Design of Tall and Special Buildings, Vol: 29, Issue: 1, pp: 1-15

Themelis, S., (2008). Pushover analysis for seismic assessment and design of structures. Doctoral Thesis, Heriot-Watt University, Edinburgh, Scotland. http://hdl.handle.net/10399/2170

Uang, C. M., (1991). Establishing R (or R w) and C d factors for building seismic provisions. Journal of Structural Engineering, Vol: 117, Issue: 1, pp: 19-28

UBC, (1997). Uniform Building Code. International Conference of Building Officials, California, USA.

Valente M., and Milani G., (2019). Damage assessment and collapse investigation of three historical masonry palaces under seismic actions. Engineering Failure Analysis, Vol: 98, Issue: 3, pp: 10-37

Vatsikas V. and Lu Y., (2003). Comparison of code-based design and performance based design procedures in earthquake engineering.

Vijayakumar, A.; Babu, D.L.V., (2012). Pushover analysis of existing reinforced concrete framed structures. European Journal of Scientific Research, Vol: 71, Issue: 2, pp: 195-202

Wei, L., and Qing Ning, L., (2012). Performance based seismic design of complicated tall building structures beyond the code specification. The Structural Design of Tall and Special Buildings, Vol: 21, Issue: 8, pp: 578-591

Wen, K. Y. and Kang, J. Y., (2001). Minimum Building Life-Cycle Cost Design Criteria. I: Methodology. ASCE Journal of Structural Engineering, Vol: 127, Issue: 3, pp: 330-337

Wen, K.Y. and Kang, J. Y., (2001). Minimum Building Life-Cycle Cost Design Criteria. II: Applications. ASCE Journal of Structural Engineering, Vol: 127, Issue: 3, pp: 338-346

Williams, A., (1997). Seismic Design of Buildings and Bridges for Civil and Structural Engineers. Dearborn Trade Publishing. 470 pages

Ye, L., and Pan Wen, (2000). The Principle of Nonlinear Static Analysis (Pushover) and Numerical Examples. Journal of Building Structures, Vol: 21, Issue: 1, pp: 37-43

Yuan, F., and X. F. Wu., (2017). Effect of load cycling on plastic hinge length in RC columns. Engineering Structures, Vol: 147, Issue: 3, pp: 90-102

Zameeruddin, Mohd and Sangle, Keshav, (2016). Seismic damage assessment of reinforced concrete structure using non-linear static analyses. KSCE Journal of Civil Engineering, Vol: 21, Issue: 4, pp: 1319-1330

Zhang, Q., Xiong, E., Liang, X., and Miao, X., (2017). Performance-based plastic design method of high-rise steel frames. Journal of Vibroengineering, Vol: 19, Issue: 3, pp: 2003-2018

Zhao, Xuemei and Wu, Yufei and Leung, A.Y.T amd Lam, Heung Fai., (2011). Plastic Hinge Length in Reinforced Concrete Flexural Members. Procedia Engineering, Vol: 14, Issue: 5, pp: 1266-1274

Zima B., (2020). Debonding Detection in Reinforced Concrete Beams with the Use of Guided Wave Propagation. Lecture Notes in Mechanical Engineering. Springer, Singapore. Proceedings of the 13th International Conference on Damage Assessment of Structures, pp: 487-497

Annexure A

4- ALL REINFORCEMENT SHALL BE DEFORMED, CONFORMING TO ASTM A-615 GRADE 60 WITH SPECIFIED YIELD STRENGTH OF NOT LESS THAN 60,000 PSI NOR MORE THAN 78,000 PSI, AND RATIO OF ULTIMATE STRENGTH / YIELD STRENGTH NOT LESS THAN 1.25.

A. GENERAL

1- NOTES GIVEN ON THIS DRAWING ARE APPLICABLE TO ALL STRUCTURAL DRAWINGS UNLESS OTHERWISE NOTED. NOTES WRITTEN ON ANY OTHER DRAWING SHALL BE APPLICABLE TO THAT PARTICULAR DRAWING ONLY UNLESS OTHERWISE CROSS REFERRED.

2- SYSTEM OF UNITS IS FPS.

3- THE CONTRACTOR SHALL BE RESPONSIBLE FOR THE SAFETY AND STABILITY OF THE STRUCTURE AND ALL TEMPORARY WORKS DURING CONSTRUCTION.

4- THE CONTRACTOR SHALL INFORM THE ENGINEER ABOUT ANTICIPATED CONSTRUCTION LOADS ON THE STRUCTURE AND OBTAIN ENGINEER'S APPROVAL THEREOF BEFORE COMMENCING WORK.

5- THE CONTRACTOR SHALL CO-ORDINATE ALL DRAWINGS OF ALL DISCIPLINES FOR ALL ITEMS INCLUDING BUT NOT LIMITED TO SIZES AND LOCATION OF ALL OPENINGS REQUIRED FOR DUCTS, PIPES AND PIPE SLEEVES, ELECTRICAL CONDUITS AND OTHER ITEMS TO BE EMBEDDED IN CONCRETE OR OTHERWISE INCORPORATED IN STRUCTURAL WORK AND SHALL BRING TO THE NOTICE OF THE ENGINEER DISCREPANCIES, IF ANY, FOR HIS INSTRUCTIONS, PRIOR TO THE START OF WORK.

6- THE CONTRACTOR SHALL PREPARE AND SUBMIT SHOP DRAWINGS AND BAR BENDING SCHEDULES FOR ENGINEER'S APPROVAL AND OBTAIN HIS APPROVAL BEFORE PROCEEDING WITH THE WORK. THE CONTRACTOR SHALL BE SOLELY RESPONSIBLE FOR THE ACCURACY OF SHOP DRAWINGS AND BAR BENDING SCHEDULES. THE ENGINEER'S APPROVAL SHALL NOT RELEVE THE CONTRACTOR FROM HIS RESPONSIBILITY.

7- THE CONTRACTOR SHALL VERIFY LAYOUT, CONFIGURATION, ALL DIMENSIONS AND LEVELS PERTAINING TO EXISTING WORKS BEFORE PROCEEDING WITH THE WORK.

8- CONTRACTOR SHALL COORDINATE SCHEDULE OF CONSTRUCTION WITH SUPPLY AND INSTALLATION OF EQUIPMENT, GLAZING WINDOW FRAMES AND OTHER ATTACHMENTS AS SHOWN ON ARCHITECTURAL DRAWING.

9- ALL LEVELS MARKED ON THE DRAWINGS ARE LEVELS OF STRUCTURAL ELEMENTS. FINISH LEVELS SHALL BE IN ACCORDANCE WITH THE ARCHITECTURAL DRAWINGS.

10- ALL MATERIALS AND WORKMANSHIP SHALL CONFORM TO SPECIFICATIONS OF THE CONTRACT. IN ABSENCE OF ANY EXPRESS OR IMPLIED SPECIFICATION IN THE CONTRACT, ALL MATERIALS AND WORKMANSHIP SHALL CONFORM TO RELEVANT AMERICAN STANDARDS.

B. FOUNDATION AND EARTHWORK.

1- FOUNDATION HAS BEEN DESIGNED FOR NET ALLOWABLE BEARING CAPACITY: 1.25 TSF FOR RAFT FOUNDATION, GEOTECHNICAL INVESTIGATION REPORT HAS BEEN PREPARED BY SWIS-TECH ENGINEERS & CONTRACTORS.

2- FOUNDATION HAS BEEN DESIGNED FOR B + G + 5 FL+ M.

3- THE CONTRACTOR SHALL BE RESPONSIBLE FOR DEWATERING SYSTEM IF AND WHERE REQUIRED DURING CONSTRUCTION.

4- TERMITE CONTROL TREATMENT SHALL BE CARRIED OUT IN THE BUILDING AS PER SPECIFICATIONS.

5- THE CONTRACTOR SHALL SUPPLY AND ERECT ADEQUATE SHORING TO SUPPORT THE SIDES OF ALL EXCAVATIONS WHERE REQUIRED TO SAFEGUARD WORKMEN AND PROTECT ANY ADJACENT STRUCTURES.

6- EXISTING UNDERGROUND SERVICES, REQUIRED TO BE LEFT IN POSITION, SHALL BE CAREFULLY PROTECTED DURING EXCAVATION AND BACKFILLING OPERATIONS.

7- WALLS OF UNDERGROUND TANK AND BASEMENT SHALL NOT BE BACKFILLED UNTIL TOP SLAB IS CAST AND CURED.

8- ANTI-TERMITE TREATMENT IS RECOMMENDED BEFORE CONSTRUCTION OF FOOTING.

C. REINFORCED CONCRETE.

1- ALL CONCRETE SHALL BE TESTED IN ACCORDANCE WITH ASTM STANDARD SPECIFICATIONS AND SHALL COMPLY WITH THE FOLLOWING REQUIREMENT. TESTING OF CLASS D & E CONCRETE SHALL BE PERFORMED IF SO DIRECTED BY THE ENGINEER.

CLASS	MIN. CYLINDER CRUSHING STRENGTH AT 28 DAYS
	psi.
A	4000
B	3000
C	3000
D	1500

2- CLASS OF CONCRETE FOR DIFFERENT COMPONENTS OF THE STRUCTURE SHALL COMPLY WITH THE FOLLOWING:

COMPONENT	COLUMNS/ PILES	SHEAR WALLS	SLABS/ BEAMS	O.H.TANK
CONCRETE CLASS	A	A	B	B
COMPONENT	REATINING WALL	FOUNDATION	LEAN 1:4:8	ALL OTHERS
CONCRETE CLASS	A	B		

3- ORDINARY PORTLAND CEMENT SHALL BE USED IN ALL CONCRETE WORKS.

4- ALL REINFORCEMENT SHALL BE DEFORMED, CONFORMING TO ASTM A-615 GRADE 60 WITH SPECIFIED YIELD STRENGTH OF NOT LESS THAN 60,000 PSI NOR MORE THAN 78000 PSI, AND RATIO OF ULTIMATE STRENGTH / YIELD STRENGTH NOT LESS THAN 1.25.

5- ALL DETAILING SHALL BE DONE AS PER ACI STANDARDS ACI-318-05 AND ACI 315.

6- CONCRETE CLEAR COVER FOR REINFORCING STEEL SHALL BE AS FOLLOWS:

CONCRETE CAST AGAINST AND	MINIMUM COVER
PERMANENTLY EXPOSED TO EARTH	3"
CONCRETE EXPOSED TO EARTH/ WATER OR WEATHER:	
BAR DIA > #6	2"
BAR DIA < #5	1 1/2"
CONCRETE NOT EXPOSED TO WEATHER OR IN CONTACT WITH GROUND:	
SLABS & WALLS	3/4"
BEAMS, COLUMNS, PRIMARY REINFORCEMENT, TIES & STIRRUPS	1 1/2"

7a- ALL REINFORCING STEEL SHALL BE HELD FIRMLY IN PLACE BEFORE AND DURING THE PLACING OF CONCRETE BY MEANS OF WIRES AND SUPPORTS ADEQUATE TO PREVENT DISPLACEMENT DURING THE COURSE OF CONSTRUCTION.

7b- AT THE TIME CONCRETE IS PLACED, REINFORCEMENT SHALL BE FREE FROM MUD, OIL, OR OTHER NON METALLIC COATINGS THAT DECREASE BOND.

7c- 1" PRE CAMBER SHALL BE PROVIDED AS AND WHEN BEAM LENGTH / SPAN IS INCREASED FROM 24' AND 1½" PRE CAMBER MUST BE PROVIDED WHEN BEAM LENGTH / SPAN WILL BE MORE THEN 36' FORM WORK SHALL REMAINED INTACT FOR 28 DAYS IN SUCH CASE.

8- BEFORE CASTING OF ANY STRUCTURAL MEMBER, THE CONTRACTOR SHALL ENSURE THAT ALL EMBEDDED ITEMS FOR ELECTRICAL, MECHANICAL, HVAC, PLUMBING, STRUCTURAL STEEL AND OTHER WORKS, AND DOWELS FOR STRUCTURAL MEMBERS AND/OR MASONARY ARE PROPERLY LOCATED IN PLACE.

9. EMBEDMENT LENGTHS

UNLESS OTHERWISE STATED ON THE DRAWINGS, THE FOLLOWING EMBEDMENT LENGTHS SHALL BE PROVIDED AS PER CODE ACI 318-11 SECTION 12.2.1.

BAR SIZE	3/8"Ø	1/2"Ø	5/8"Ø	3/4"Ø	1"Ø
EMBEDMENT LENGTH BEAM	17"	22"	26"	33"	55"
EMBEDMENT LENGTH COLUMN	15"	19"	24	29"	48"

10. LAP LENGTH

UNLESS OTHERWISE STATED ON THE DRAWING,THE FOLLOWING LAP LENGTHS SHALL BE PROVIDED AS PER CODE ACI 318-11SECTION 12.2.1.

BAR SIZE	3/8"Ø	1/2"Ø	5/8"Ø	3/4"Ø	1"Ø
LAP LENGTH BEAM	22"	29"	36"	43"	72"
LAP LENGTH COLUMN	19"	25"	32"	36"	62"

EXCEPT WHEN OTHERWISE SHOWN ON THE DRAWING, WHENEVER REINFORCING BARS OF DIFFERENT SIZES ARE TO BE SPLICED,LAP LENGTH SHALL BE LARGER OF Ld OF LARGER BAR & TENSION LAP SPLICE LENGTH OF SMALLER BAR

11- DEVELOPMENT LENGTH OF 90° HOOKS SHOULD BE 17db AND SHOULD BE ANCHORED IN CONFINED CORE OF COLUMN.

12- CONSTRUCTION JOINTS NOT SHOWN ON THE DRAWINGS SHALL BE SO MADE AND LOCATED AS TO LEAST IMPAIR THE STRENGTH OF THE STRUCTURE AND SHALL NEED PRIOR APPROVAL OF THE ENGINEER. IN GENERAL THEY SHALL BE LOCATED NEAR THE MIDDLE OF THE SPAN OF SLABS AND BEAMS. JOINTS IN COLUMNS SHALL BE AT THE UNDERSIDE OF FLOORS, SLABS OR BEAMS AND AT THE TOP OF FOOTINGS OR FLOOR SLABS. JOINTS SHALL BE PERPENDICULAR TO MAIN REINFORCEMENT. ALL REINFORCING STEEL SHALL BE CONTINUED ACROSS JOINTS.

13- FLOOR SLABS SUBJECT TO VEHICULAR TRAFFIC SHALL BE TREATED WITH APPROVED METALLIC FLOOR HARDENER.

14. CONSTRUCTION JOINTS

SURFACE OF CONCRETE CONSTRUCTION JOINTS SHALL BE CLEANED AND LAITANCE REMOVED.

IMMEDIATELY BEFORE NEW CONCRETE IS PLACED, ALL CONSTRUCTION JOINTS SHALL BE WETTED AND STANDING WATER REMOVED.

BEAMS, GIRDERS, OR SLABS SUPPORTED BY COLUMNS OR WALLS SHALL NOT BE CAST OR ERECTED UNTIL CONCRETE IN THE VERTICAL SUPPORT MEMBERS IS NO LONGER PLASTIC.

D- BRICK MASONRY WORKS

1- ALL MASONRY DESIGN AND CONSTRUCTION SHALL CONFORM TO 530-02/ASCE 5-02. LOCAL AUTHORITY REQUIREMENTS AND SPECIFICATIONS. EQUIVALENT BRITISH STANDARDS MAY BE CONSIDERED SUBJECT TO APPROVAL OF THE EMPLOYER. CONSULTANT.

2- THE CONTRACTOR IS TO TAKE PARTICULAR CARE THAT ALL THE PERPENDS AND BEDS ARE PROPERLY FILLED WITH MORTOR.

3- ALL CONTROL JOINTS SHALL BE FILLED WITH COMPRESSIBLE EXPANDABLE FILLER. REFER TO SPECIFICATIONS FOR FIRE RATED WALLS.

4- FIRE RATING, SOUND AND THERMAL INSULATION PROPERTIES SHALL BE IN ACCORDANCE WITH THE PROJECT SPECIFICATIONS.

5- PROVIDE LINTELS OVER ALL OPENING OR RECESSES IN MASONRY WALLS INCLUDING THOSE FOR MECHANICAL OR ELECTRICAL SERVICES OR EQUIPMENT, SEE STANDARD DETAIL DRAWINGS FOR LINTEL SIZES AND DETAILS.

6- PROVIDE RESTRAINT TO ALL MASONRY WALLS AT SLAB SOFFIT AND SIDES AS SHOWN IN STANDARD DETAIL DRAWINGS.

7- ALL MASONRY ANCHORS, MASONRY TIES AND EMBEDDED ITEMS SHALL BE HOT DIP GALVANIZED.

E. PROPS, FORMWORK AND CURING.

1- SEQUENCE OF REMOVAL OF FORMWORK SHALL BE AS APPROVED BY THE ENGINEER.

2- ALL PROPS, BRACINGS, GUY WIRE PROPS, ETC. REQUIRED FOR STRENGTH AND STABILITY OF THE STRUCTURE AND THE FORMWORK DURING CONSTRUCTION SHALL BE PROVIDED BY THE CONTRACTOR.

3- AT LEAST ONE LOWER FLOOR SHALL REMAIN PROPPED UNTIL THE UPPER FLOOR IS CAST AND CURED.

F. OPENINGS,CONCEALED CABLES AND CAST -IN CONDUITS

1. NO HOLES OR CHASES ARE PERMITTED IN CONCRETE MEMBERS OTHER THAN THOSE AS DETAILED IN THE STRUCTURE DRAWINGS OR AUTHORIZED BY THE ENGINEER PRIOR TO CONCRETING
2. NO HACKING OR CORING OF STRUCTURE IS PERMITTED WITHOUT PRIOR WRITTEN APPROVAL FORM THE ENGINEER.
3. PRIOR TO CONSTRUCTION THE CONTRACTOR SHALL COORDINATE ALL STRUCTURAL, ARCHITECTURAL AND MECHANICAL & ELECTRICAL (M&E) DRAWINGS FOR OPENINGS, CONCEALED CABLES AND CAST –IN CONDUITS AND FITTINGS. THE CONTRACTOR SHALL INFORM THE ENGINEER IMMEDIATELY OF ANY DISCREPANCIES IN DRAWINGS PRIOR TO CONSTRUCTION.
4. LOCATION ,MAXIMUM SIZE AND MINIMUM SPACING OF EMBEDDED PIPE AND CONDUITS IN R.C SLAB.

5. CONDUITS, PIPES, AND SLEEVES PASSING THROUGH A SLAB WALL, OR BEAM SHALL NOT IMPAIR SIGNIFICANTLY THE STRENGTH OF THE CONSTRUCTION.

FIGURE A.1